Lawiey
IN-36-CR
237033
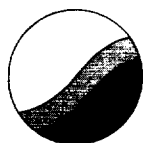*61P*

MARYLAND

COLLEGE PARK CAMPUS

NCCI-25

PROGRESS OF RESEARCH ON WATER VAPOR LIDAR

by

T. D. Wilkerson and U. N. Singh
Atmospheric Lidar Observatory
Institute for Physical Science and Technology
University of Maryland, College Park, MD 20742

BN-1104

October 1989

INSTITUTE FOR PHYSICAL SCIENCE AND TECHNOLOGY

PROGRESS OF RESEARCH ON WATER VAPOR LIDAR[1]

by

T. D. Wilkerson and U. N. Singh
Atmospheric Lidar Observatory
Institute for Physical Science and Technology
University of Maryland, College Park, MD 20742

ABSTRACT

Research is summarized on applications of stimulated Raman scattering (SRS) of laser light into near infrared wavelengths suitable for atmospheric monitoring. Issues addressed are conversion efficiency, spectral purity, optimization of operating conditions, and amplification techniques.

A Raman cell was developed and built for the laboratory program, and is now available to NASA-Langley, either as a design or as a completed cell for laboratory or flight applications. The Raman cell has been approved for flight in NASA's DC-8 aircraft. The "self-seeding" SRS technique developed here is suggested as an essential improvement for tunable near-IR DIAL applications at wavelengths of order 1 μm or greater.
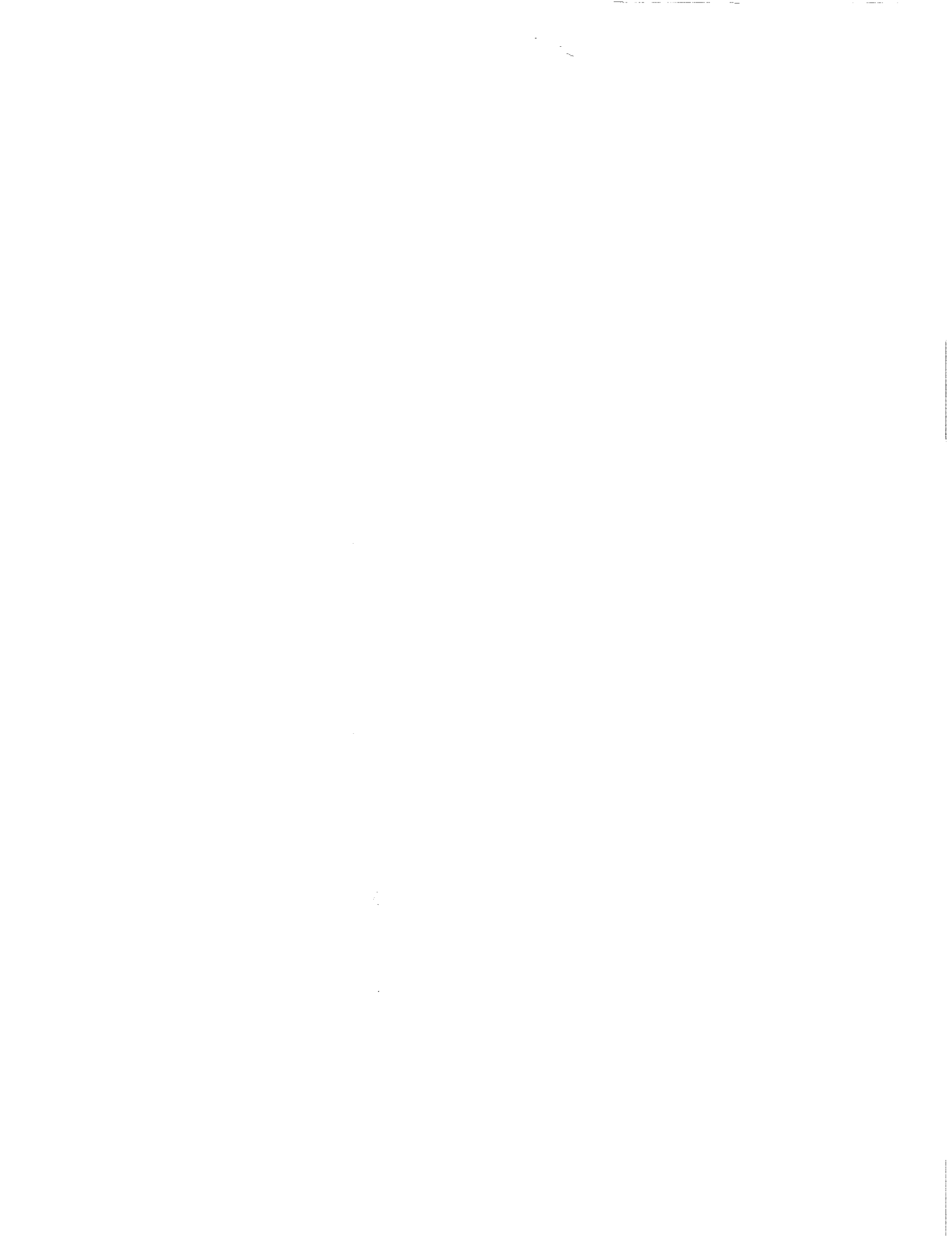
PROGRESS OF RESEARCH ON WATER VAPOR LIDAR

For atmospheric monitoring of water vapor by the DIAL technique when the abundance of H_2O is low—as in the stratosphere, or in the polar troposphere—*efficient* lidar operation is required in the 940 nm or 1140 nm absorption bands of water vapor. Moreover, *narrow line* optical transmission is required because of the small H_2O linewidth (HWHM ~ 0.1 cm^{-1} at sea level, ~ 0.015 cm^{-1} (Doppler) at low atmospheric pressure.

Because these wavelengths are hard to reach by any pulsed laser method, we have investigated their generation (e.g., 940 nm) by the stimulated Raman scattering (SRS) technique, using a narrow line tunable laser (~ 676 nm) as the pump source at shorter wavelength, the beam being single-passed through high pressure H_2 in which the first Stokes shift is about 4100 cm^{-1}. Following a preliminary study[2] we have worked on two essential aspects of SRS applications: optimization of output energy, and suitability of the output line spectrum for quantitative DIAL measurements in the atmosphere. Results are given in detail in the reports reproduced in Appendices A & B. For an especially demanding test of the narrowness of tunable line radiation, we elected to utilize the O_2 A-band absorption spectrum[3] near 760 nm, because the O_2 lines have HWHMs ~ .03-.05 cm^{-1} under ambient conditions. We found that the narrow line character of our tunable laser light near 585 nm was, as expected, preserved in the SRS process producing output at 760 nm. This exercise will be repeated for 940 nm in coming months.

Also, we have extended the SRS work to yet longer wavelength, to bracket

---

[2] B. E. Grossmann, U. N. Singh, N. S. Higdon, L. J. Cotnoir, T. D. Wilkerson and E. V. Browell, *Appl. Opt.* **26**, 1617 (1987).

[3] K. J. Ritter and T. D. Wilkerson, *J. Molec. Spectrosc.* **121**, 1 (1987).

the wavelength regions (~ 1140 nm) that will ultimately have to be covered for complete water vapor work in the atmosphere. To do this, we employed the Nd:YAG fundamental (~ 200 mJ at 1.064 μm) as the pump source, generating 1.54 μm as the first Stokes output in methane (see Appendices C & D). In so doing, we first verified that the SRS applications indeed become significantly more difficult at long wavelength. We devised a way of overcoming the threshold and conversion efficiency problems—namely to feed back the ordinarily wasted "backward Raman" radiation as a "seed" for the forward Raman process. The latter result holds very favorable indications for near infrared SRS processes generally, and may make a vital difference in the conversion efficiency from pump radiation at 773 nm (e.g., alexandrite or Ti:Al$_2$O$_3$) to 1140 nm using H$_2$ as the Raman medium. This wavelength region is now well bracketed by successful SRS conversion schemes at both shorter and longer wavelength.

Consistent with the intent of the Cooperative Agreement NCC 1-25, all of the technology developed in this program is available to the Water Vapor Lidar program at NASA-Langley Research Center, including a high pressure Raman cell if that is needed for laboratory or flight operations.[4] The subject grant supported all of the 940 nm work, plus parts of the 1.54 μm study that were deemed a good investment in researching how to carry out SRS applications to water vapor measurements beyond 1 μm wavelength.

All of the 940 nm work reported here was completed by July 31, 1989. The essentials of the self-seeding SRS work were worked out by that time, and some of the results and analysis were then refined in August and September.

Details of the research results are given in the journal articles and

---

[4]A bonus for the program is that the Raman cell design and construction has been approved for flight on NASA's DC-8 aircraft, as a part of the NASA-Goddard aerosol experiment for the GLOBE project.

presentation abstracts included as Appendices A-D to this report. References for these documents are given below. This completes the current description of research progress under NCC 1-25.

APPENDICES

A. U. N. Singh, Z. Chu, R. Mahon, and T. D. Wilkerson, "Raman-shifted Radiation for Lidar Applications", *Proc. Conf. on Lasers and Electro-Optics (CLEO '89)*, Baltimore, MD (April, 1989).

B. U. N. Singh, Z. Chu, R. Mahon, and T. D. Wilkerson, "Optimization of a Raman-shifted Dye Laser System for DIAL Applications", submitted to *Applied Optics* (May, 1989).

C. Z. Chu, U. N. Singh, and T. D. Wilkerson, "A Self-Seeded SRS System for the Generation of 1.54 μm Eye-Safe Radiation", to be published in *Optics Communications* (1990).

D. U. N. Singh, Z. Chu, and T. D. Wilkerson, "Efficient Near-IR Light Source for Eye-Safe Lidar Applications", *Proc. Optical Remote Sensing of the Atmosphere* (1990), OSA meetings, Incline Village, NV (February 1990).

APPENDIX A

Raman-shifted Radiation for Lidar Applications[*]

U.N. Singh, Z. Chu, R. Mahon, and T.D. Wilkerson

University of Maryland

Institute for Physical Science and Technology

College Park, MD 20742-2431

Tel: (301) 454-4760, (301) 454-5401

Abstract

An efficient Raman-shifted dye laser system emitting narrowband (~ 0.03 cm^{-1}), tunable radiation at 765 and 940 nm for DIAL applications, and a Raman-shifted Nd:YAG laser system at 1.54 μm for eye-safe aerosol lidar measurements, are described.

Raman-shifted Radiation for Lidar Applications[*]

U.N. Singh, Z. Chu, R. Mahon, and T.D. Wilkerson

University of Maryland

Institute for Physical Science and Technology

College Park, MD 20742-2431

Tel: (301)-454-4760, (301) 454-5401

Summary

Differential Absorption Lidar (DIAL) measurements in the water vapor bands (730 and 940 nm) and the A-band of molecular oxygen (760-770 nm) have been suggested[1-3] for profiling atmospheric properties such as humidity, temperature, pressure, and density. For this purpose, intense pulsed laser sources of tunable, narrowband radiation in the near infrared are necessary. Because similar lasers are available in the visible spectrum, stimulated Raman scattering is one of the most efficient methods for frequency shifting radiation for use in the near infrared. In particular Nd:YAG-pumped dye lasers perform well in the 560-700 nm range but their efficiency falls off rapidly above 700 nm. Higher energy outputs can be achieved by Raman shifting visible wavelengths into infrared radiation at the first Stokes frequency. The requisite tunability and spectral purity of the output is derived from the dye laser input. Hydrogen is especially suitable as a Raman conversion medium because it is characterized by having the largest frequency shift (4155 cm^{-1}) in a single Stokes order, high gain, and very small collision broadening[4].

An experiment diagram is shown in Fig 1. A frequency-doubled, Nd:YAG-pumped dye laser[4] emitted narrowband radiation (≤ 0.02 cm^{-1}) at 577-583 and 676 nm. The first Stokes radiation at 760-770 and 940 nm, respectively, was generated in a 1-meter long, single pass Raman cell containing hydrogen.

Raman-shifted Radiation

U.N. Singh, Z. Chu, R. Mahon, T.D. Wilkerson

To carry over the narrow bandwidth of the dye laser to the Raman-shifted wavelength, we operated the Raman cell at pressures below 14 atm. The first Stokes conversion was optimized by monitoring the resultant pulse energy for three pump beam focussing geometries. We attained energy conversion efficiencies of 45% and 37% at 765 and 940 nm, respectively.

We utilized the P-branch of the oxygen "A-band" to test the spectral purity of both the dye laser and Raman-shifted dye laser radiation at 760-770 nm. Optical depth measurements were made at the centers of 25 lines in the P-branch of the oxygen A-band in air at NTP, contained in a White cell of 60 meter path length. Fig. 2 shows results for 760-770 nm radiation generated directly in the dye laser (*), and Fig. 3 represents the use of dye laser light Raman-shifted from ~ 580 nm (+). The solid line at 45° is the calculated optical depth using line parameters from Ritter and Wilkerson[5] that were obtained with highly monochromatic light from a CW dye laser. The dotted lines represent the theoretical optical depth corrected for frequency stability and finite linewidth of the pulsed radiation. The data and theoretical calculations agree, indicating a high degree of spectral purity, and thus the feasibility of using the Raman-shifted radiation for DIAL measurements.

We are also studying the generation of 1.54 μm radiation by Raman-shifting the output of a Nd:YAG laser at 1.06 μm in a Raman cell containing methane ($\delta\nu = 2987$ cm^{-1}). This radiation will be used for aerosol lidar measurements that are relatively eye-safe. Optimization results will be presented.

Raman-shifted Radiation

U.N. Singh, Z. Chu, R. Mahon, T.D. Wilkerson

1. E.V. Browell, T.D. Wilkerson, and T.J. McIlrath, Appl. Opt., 18, 3473 (1979).

2. T.D. Wilkerson and G.K. Schwemmer, Opt. Eng., 21, 1022 (1982).

3. C.L. Korb and C.Y. Weng, J. Appl. Meteor., 21, 1346 (1982).

4. B.E. Grossmann, U.N. Singh, N.S. Higdon, L.J. Cotnoir, T.D. Wilkerson, and E.V. Browell, Appl. Opt., 26, 1617 (1987).

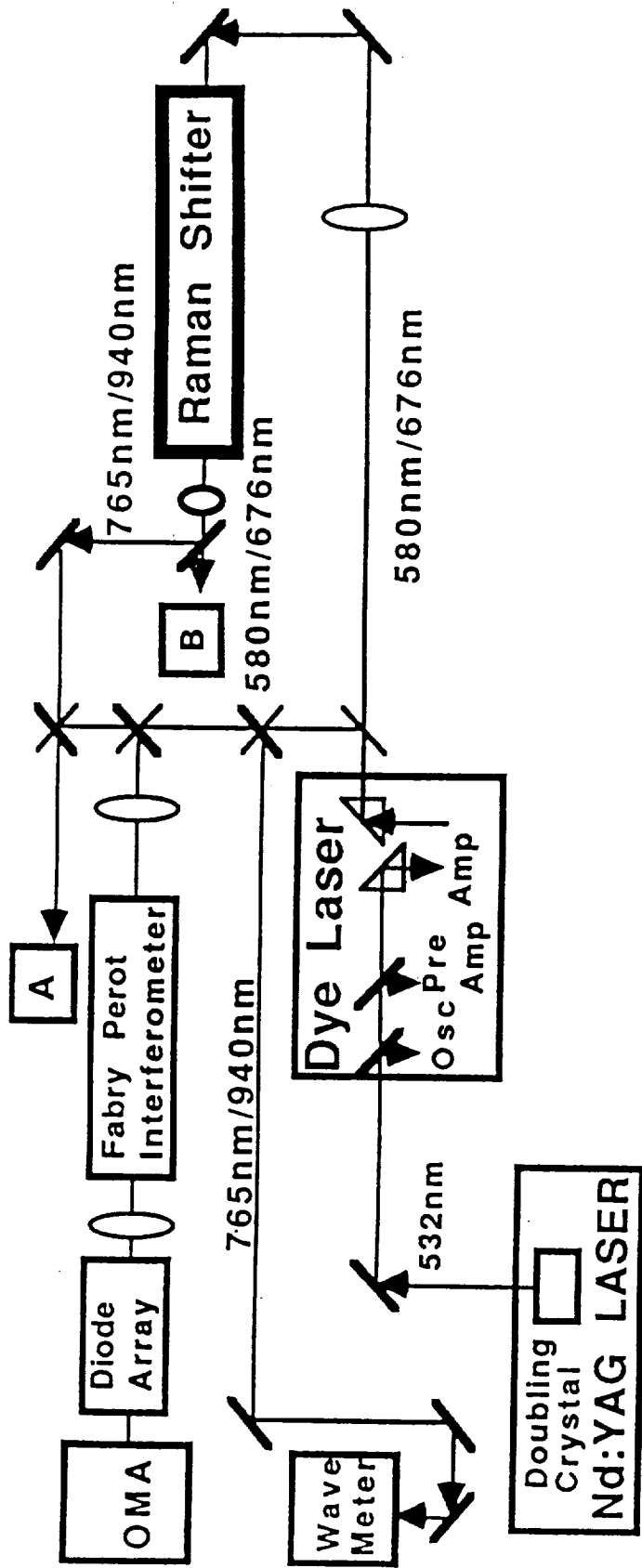5. K. Ritter and T.D. Wilkerson, J. Mol. Spectro., 121, 1 (1987).

Raman Shifter

765nm/940nm

580nm/676nm

580nm/676nm

B

A

765nm/940nm

Fabry Perot Interferometer

Diode Array

OMA

Wave Meter

Dye Laser

Osc Pre Amp Amp Amp

532nm

Doubling Crystal

Nd:YAG LASER

Fig. 1 A diagram of the experimental apparatus is shown for the first Stokes

generation of 765 and 940 nm radiation.
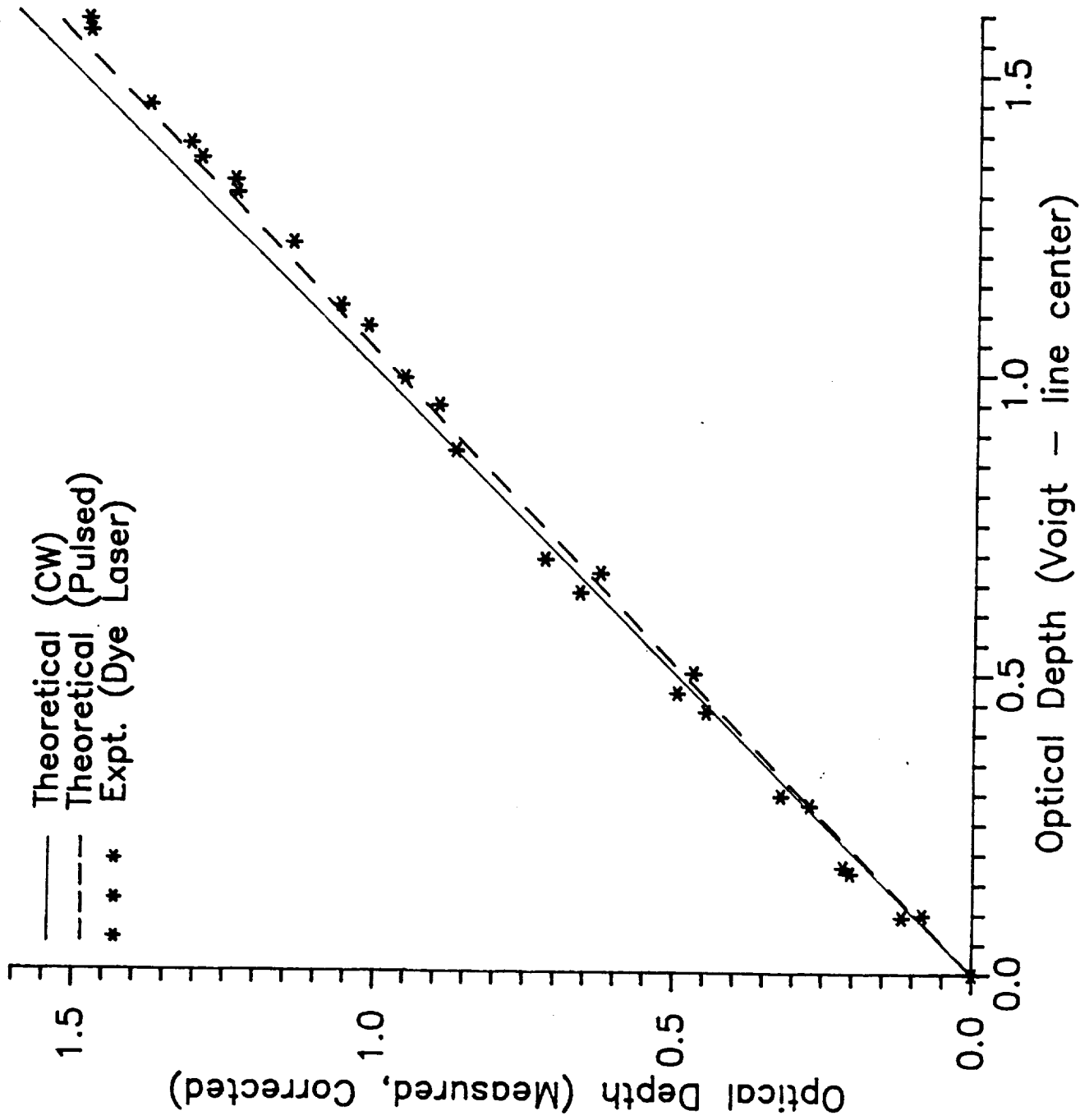
Oxygen Absorption Measurements (A—Band)

Theoretical (CW)
Theoretical (Pulsed)
Expt. (Dye Laser) * * *

Optical Depth (Voigt — line center)

Optical Depth (Measured, Corrected)

Fig. 2 Optical depth measurements with 760-770 nm radiation generated directly in the dye laser.

Oxygen Absorption Measurements (A—Band)

Theoretical (CW)
Theoretical (Pulsed)
+++ Expt. (Raman Shifted)

Optical Depth (Voigt — line center)
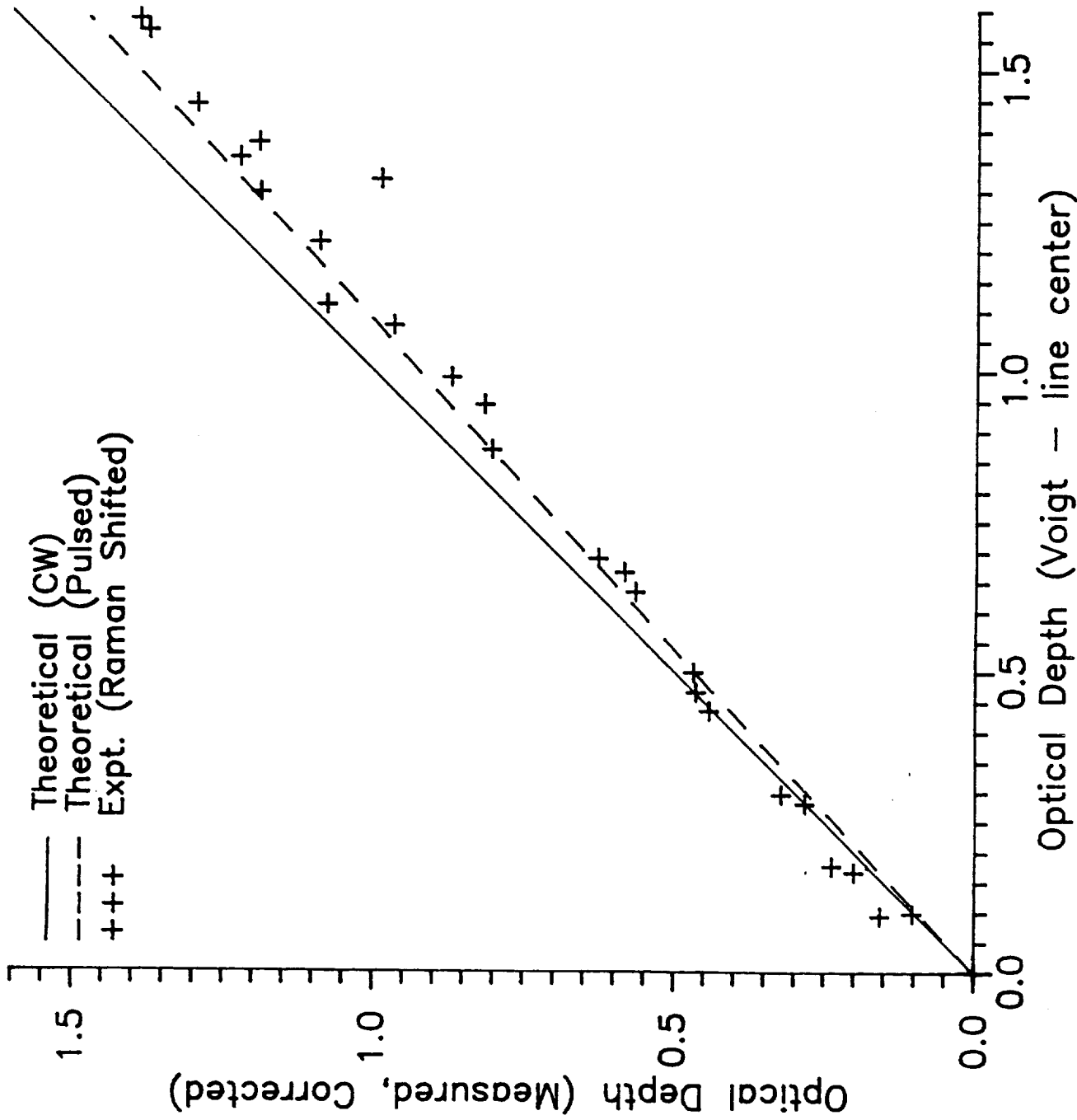
Optical Depth (Measured, Corrected)

Fig. 3 Optical depth measurements with 760-770 nm radiation generated through Raman-shifting the dye laser radiation.

APPENDIX B

OPTIMIZATION OF A RAMAN SHIFTED DYE LASER SYSTEM
FOR DIAL APPLICATIONS

Upendra N. Singh, Zhiping Chu, Rita Mahon and Thomas D. Wilkerson
University of Maryland
Institute for Physical Science and Technology
College Park, Maryland 20742-2431

ABSTRACT

We describe an efficient Raman-shifted dye laser system that generates tunable radiation at 765 and 940 nm with a bandwidth of 0.03 cm^{-1}. Operating a Raman cell at hydrogen pressure below 14 atm, we recorded optimum first Stokes energy conversions of 45% and of 37% at 765 and 940 nm, respectively. Optical depth measurements made at the centers of 25 absorption lines in the P-branch of the oxygen A-band imply a high spectral purity for both the laser and the Raman-shifted radiation, and thus indicate the feasibility of using the stimulated Raman-scattered radiation for differential absorption lidar (DIAL) measurements.

I. INTRODUCTION

In recent years various differential absorption lidar (DIAL) measurements in the water vapor bands (730 and 940 nm) and the A-band of molecular oxygen (750 - 770 nm) have been suggested,[1-8] and in some cases demonstrated, as a means of profiling tropospheric and stratospheric variables such as humidity, temperature, pressure and density. For this purpose, intense laser sources of pulsed, tunable, and narrow band radiation in the near infrared are necessary.

Existing differential absorption lidar (DIAL) systems for measuring water vapor in the troposphere operate at wavelengths near 720 nm.[1-3] Absorption lines in this spectral region are strong enough that ambient concentration levels of water can be measured using DIAL techniques with range resolutions of the order of 30 meters or more. To extend accurate DIAL operations to the upper troposphere, as well as the lower stratosphere and the polar regions where the water vapor content is much reduced, strong absorption bands near 940 and 1140 nm[9] must be used. The lines in these bands are, respectively, about 15 and 35 times stronger than those in the 720 nm band. Lidar systems working at these longer wavelengths will also be required for space-borne operations.[10]

Since high power, tunable, laser sources are available in the visible spectral range, stimulated Raman scattering is one of the most efficient methods for frequency-shifting radiation for use in the infrared. In particular, Nd:YAG-pumped dye lasers perform very well in the 560 - 700 nm range but their efficiency falls off rapidly for wavelengths above 700 nm. Higher energy outputs can be achieved at these longer wavelengths by Raman-shifting a visible wavelength laser to generate radiation at the first

2

Stokes frequency. The necessary tunability is inherent in the dye laser used to pump the Raman cell. In carrying out such experiments, one also learns how to optimize the "Raman shifting" processes for other tunable, pulsed lasers such as titanium-doped sapphire.

The interpretation of DIAL measurements[11] generally requires laser linewidths having a full width at half maximum (FWHM) of less than 0.03 cm^{-1}. In order to retain this narrow a linewidth one is restricted to using Raman media having small collision broadening coefficients such as hydrogen and deuterium.[12-13] Previous experimental studies of the spectral linewidth of the first Stokes radiation produced in stimulated Raman scattering (SRS) in hydrogen showed that the linewidth requirement puts an upper limit of 14 atm[14] on the allowable hydrogen pressure. Here, we describe the experimental optimization for producing the first Stokes at 765 and 940 nm with the necessary 0.03 cm^{-1} bandwidth. We also report optical depth measurements made at the line centers of 25 absorption lines in the P-branch of the oxygen A-band (760 - 770 nm) that indicate a high degree of spectral purity for both the dye laser and the Raman-shifted dye laser radiation.

II. EXPERIMENT

A schematic diagram of the experiment is shown in Fig. 1. A frequency-doubled, Nd:YAG-pumped dye laser[15] generated narrow band radiation of bandwidth $\leq$ 0.02 cm^{-1} tunable between 577 and 583 nm and at 676 nm. The 1st Stokes radiation was generated in a 1 meter long, single pass Raman cell containing hydrogen gas. We located the beam waist of the pump beam at the center of the cell in order to keep the power density on the windows to a minimum. The linewidth of the dye laser output and the first Stokes radiation

were measured with a Fabry-Perot interferometer, while a wavemeter recorded the absolute wavelengths. An optical multichannel analyzer and a linear photodiode array were used for continuous monitoring of the spectral mode output of the laser and Raman shifted radiation, and were also used to measure the linewidth. The same arrangement was used to observe the cross section of the spatial profile of the laser and its Raman-shifted output. The first Stokes radiation was separated from the pump light, and any higher order Stokes and anti-Stokes radiation present, by using two dichroic mirrors together with a colored glass filter and a narrowband interference filter. All measurements of energy and conversion efficiency were made using two pyroelectric probes connected to an energy ratiometer.

III. STOKES CONVERSION EFFICIENCY AT 765 AND 940 NM

For optimal conversion of visible dye laser radiation into light at the first Stokes frequency, a Raman self-generator was operated above the stimulated Raman threshold and in the regime of finite pump depletion, but below the threshold for second Stokes generation. Since we needed to preserve the narrow laser linewidth, there was an upper limit on the gas pressure that could be used in the Raman cell. It was long accepted that, in the non-saturated regime, the energy of the generated first Stokes was independent of the confocal parameter of the pump, so long as the confocal parameter was smaller than the length of the Raman-active medium. However, the threshold for Stokes generation was found to depend strongly on the pump confocal parameter[16] due to the influence of the Stokes and anti-Stokes coupling, the threshold increasing as the pump confocal parameter decreased.

In order to avoid the gain suppression experienced by the first Stokes

4

radiation, it is necessary to keep the pump beam angles within the phase matching angle, which is about 5 mrad at 14 atm of hydrogen at 765 nm. In addition, at pump levels above saturation, it is also necessary to keep the first Stokes beam within the phase matching angle for producing second Stokes radiation by four-wave mixing. The second (and higher) order Stokes radiation can be produced by four-wave mixing of the original pump and the first Stokes radiation with a conical emission maximized at the phase-matching angle, which is of the order of 5.5 mrad for hydrogen at 14 atm.[17] All of these considerations indicate that a collimated geometry would result in an optimised conversion to the first Stokes light. Hence the first Stokes Raman conversion efficiency was measured as a function of the pump beam confocal parameter, the pressure of hydrogen, and of the pump energy. Due to the necessity of retaining the narrow linewidth for DIAL measurements, the first Stokes conversion efficiency was optimized for a hydrogen pressure of 14 atm. The conversion efficiency was found to increase as the pump beam confocal parameter was increased from 0.5 to 10 cm and also showed a linear dependence on pump energy as the pump energy was increased over the range of 5 to 30 mJ.

The first Stokes light generated at 765 nm is seen in Fig. 2(a) to reach a 45% energy conversion efficiency (58% quantum efficiency). This output was achieved using 20 mJ of pump energy at 580 nm, focussed into a cell containing hydrogen at 14 atm, using a 2 meter focal length lens to produce a pump beam having a confocal parameter of about 10 cm. Likewise, the measurements for generating 940 nm radiation are shown in Fig. 2(b). The energy conversion efficiency to 940 nm reaches 37% (53% quantum efficiency), when 25 mJ of pump energy at 676 nm are focussed in the same geometry.

Increasing the hydrogen cell pressure gave rise to an increase in the

first Stokes conversion efficiency in both cases. As can be seen in figure 2(a) and 2(b), this efficiency at 765 and 940 nm reached values of 52% and 42%, respectively, for a hydrogen pressure of 28 atm. This higher conversion efficiency at higher pressure was significant, but linewidth measurements indicated a linewidth too broad to be useful in DIAL applications. The decrease in the conversion efficiency at higher wavelength (940 nm) compared to shorter wavelength (765 nm) is expected due to the wavelength dependence of the Raman gain coefficient.

The first Stokes energy produced at 765 and at 940 nm is shown in Fig. 3 as a function of pump energy for two pump geometries and a fixed cell pressure of 17 atm. In general, for a given focussing geometry and at a fixed pressure of hydrogen, the first Stokes energy increases linearly for increasing pump energies in the range of 10 to 30 mJ. Measurements at the second Stokes frequency showed a negligible generation even at the highest pump levels. The backward Stokes conversion efficiency at 940 nm, is shown in Fig. 4 as a function of pressure for different pump geometries. The backward Stokes component increases with increasing pressure, while it decreases with increased confocal parameter. With a 2 meter focal length lens, the backward Stokes conversion efficiency was measured to be less than 1% at 14 atm of hydrogen.

IV. LINEWIDTH MEASUREMENT

The linewidths of the dye laser output and of the first Stokes radiation were measured with a Fabry-Perot interferometer with a free spectral range of 0.2 cm^{-1}. Interferometer plates coated for the appropriate wavelengths were used, and the fringes were imaged on a linear photodiode array and recorded

using an optical multichannel analyzer. A krypton-ion laser-pumped, high resolution cw dye laser operating between 720 - 760 nm was used to check that the resolution of the Fabry-Perot plates was sufficient to conduct linewidth measurements in the range of 0.02 cm^{-1}. The effective finesse was determined to be about 50 corresponding to the resolution of the plates being 0.004 cm^{-1} for a free spectral range of 0.2 cm^{-1}.

The dye laser linewidth at 580 and 676 nm was measured to be 0.02 cm^{-1}. The first Stokes linewidth at 765 and 940 nm was measured to be 0.03 cm^{-1} at 14 atm, and 0.05 cm^{-1} at 28 atm of hydrogen. The Raman line broadening at higher hydrogen pressure was the main reason that we had to optimize the Raman conversion efficiency at 14 atm, for practical applications of DIAL involving narrow lines of water vapor in the atmosphere.

V. SPECTRAL PURITY ESTIMATION IN THE OXYGEN A-BAND (760-770 NM)

Electronic transitions in the P-branch of the oxygen A-band [$b^1\Sigma^+$(v=0) ← $x^3\Sigma^-$(v=0)]were used to estimate the spectral purity of both the dye laser and Raman shifted dye laser radiation at 760-770 nm. The very narrow absorption lines of this band provide a high spectral contrast with which to assess the spectral purity of the laser or Raman-shifted light. These lines and other features of the oxygen A-band and B-band have been proposed, and in fact, made use of in a wide variety of remote sensing methods.[4-7,18]

The DIAL measurements of atmospheric pressure are made by measuring the absorption of the on-line laser in a trough region between strong absorption lines in the R-branch of the band,[6] whereas atmospheric temperature can be obtained via the absorption of the on-line laser when centered on a narrow, high excitation line in the P-branch.[5] The width of these lines at sea level

atmospheric pressure is between 0.06 and 0.1 cm^{-1}. Thus for a ground based

DIAL measurement the laser bandwidth should be small with respect to the

absorption linewidth, e.g. 0.02-0.03 cm^{-1} (or less, for high altitude).

Besides the tunability and linewidth requirements, the DIAL measurements are

extremely sensitive to the presence of any amplified spontaneous emission

(ASE). The ASE, being broad band in nature and outside the nominal laser

bandwidth, results in a non-absorbed component when such a laser is tuned onto

the central frequency of absorption lines. This can be seen from the optical

depth measurement at a specific absorption line by using the differential

principle of the measurement (B/A) where A is the fraction of the input energy

to the absorption cell and B is the output energy from the cell. The optical

depth at the center of the absorption line is given by the Beer-Lambert Law:

$$\tau_0 = -\ell n\left(\frac{(B/A)_{min}}{(B/A)_{max}}\right) \tag{1}$$

where $(B/A)_{min}$ and $(B/A)_{max}$ are ratios of the transmitted energy to the

incident energy both on and off line center. In the presence of any broadband

radiation, such as ASE, in the incident light, the optical depth at line

center will be given by

$$\tau_0 = -\ell n\left[\frac{(B/A)_{min,\delta} + (B/A)_{ASE}}{(B/A)_{max,\delta} + (B/A)_{ASE}}\right] \tag{2}$$

where δ indicates a narrowband component and ASE refers to any broadband

component. In the limit of $(B/A)_{ASE} \ll (B/A)_{max,\delta} \simeq (B/A)_{max}$ the optical depth

can be approximated by:

$$\tau_0 \simeq -\ell n\left[\frac{(B/A)_{min}}{(B/A)_{max}} + \frac{(B/A)_{ASE}}{(B/A)_{max}}\right] \tag{3}$$

broadband, the second term of Eqn (3) contributes significantly. The actual backscattered signal would be twice the expected backscattered signal (100% error) for a measurement altitude for which 99% of the narrowband energy has been absorbed by the oxygen absorption feature.

The White cell used for measuring the transmission at the line center consisted of two 30 cm diameter, high reflectivity mirrors, having a 4.8 meter radius of curvature, and air-spaced by 1.63 meter. The path length was typically 60 m and could be adjusted in increments equal to twice the mirror separation by changing the insertion angle of the beam into the mirror geometry. The incident laser energy was monitored, and the transmission through the cell was determined using two pyroelectric detector probes connected to an energy ratiometer. By taking the ratio of the transmission at the line center to that at the line edge, the differential transmission of each line was measured.

We measured the transmission at the centers of 25 lines in the P-branch of the oxygen A-band in air at NTP contained in a White cell of 60 m path length. The measured optical depth, τ_j, at the center of the j-th line is given by:[19]

$$\tau_j = -\ell n(T_j/B_j) \tag{4}$$

where $T_j = \dfrac{(B/A)_{min}}{(B/A)_{max}}$ is the measured optical transmission at the j-th line center, and B_j is an averaged base line correction. Measurements shown in Fig. 5 correspond to the optical depths measured using the 760-770 nm dye laser radiation(*), and those presented in Fig. 6 correspond to the use of Raman-shifted dye laser radiation.(+)

To ascertain the suitability of these laser and laser/SRS outputs for

DIAL applications requiring stable, narrow line radiation, we calculated the expected optical depth for each of the 25 lines using the O_2 line strength and width data from Ritter and Wilkerson.[20] The latter had been obtained using a stabilized CW dye laser having a very narrow frequency spread of $10^{-4} cm^{-1}$. The values calculated in this way could, in principle, differ greatly from the values measured with the pulsed light sources if the latter were of significantly poorer quality as regards finite linewidth, frequency jitter arising from the intracavity etalon, amplified spontaneous emission in the dye laser output, or frequency redistribution in the SRS process.

Without regard to these phenomena, agreement between measured and expected optical depths would appear as a $45°$ line in Figures 5 and 6. However, the appropriate comparisons in these figures are indicated by the dashed lines that represent a realistic accounting for the finite linewidth and the small frequency jitter of the dye laser. This correction is justified because the measured optical depth is an average of the O_2 line profile (Voigt) weighted by the laser frequency distribution.

To make this calculation as accurate as possible, we made frequency stability measurements using a wavemeter[21] with a high resolution Fizeau wedge that indicated a frequency stability of order 0.007 cm^{-1}. The linewidth of the first Stokes output at 760 nm (0.03 cm^{-1}) was slightly larger than the linewidth of the dye laser (0.02 cm^{-1}) in the same wavelength range. No significant broadband ouput (i.e., ASE) was detected. The average optical depth at the line center, $\bar{\tau}_0$, is given by:

$$\bar{\tau}_0 = -\ell n \int_{-\infty}^{+\infty} G(\nu-\nu_0) \exp[-\tau(\nu-\nu_0)] \, d(\nu-\nu_0) \tag{5}$$

where a Gaussian frequency distribution, $G(\nu-\nu_0)$, is assumed. The optical depth distribution $\tau(\nu-\nu_0)$ is defined as[19]

$$\tau(\nu-\nu_0) = S_0 \, L \, n \, V(\nu-\nu_0) \tag{6}$$

where S_0 is the line center strength, L is the absorption path length, n is the oxygen number density and $V(\nu-\nu_0)$ is the absorption line profile which is a Voigt function. Thus equation (4) can be written as

$$\bar{\tau}_0 = -\ell n \int_{-\infty}^{+\infty} G(\nu-\nu_0) \, \exp[-S_0 \, L \, n \, V(\nu-\nu_0)] \, d(\nu-\nu_0) \tag{7}$$

The dotted line in Fig. 5 represents the calculated optical depth, τ_0 for the dye laser linewidth of 0.02 cm^{-1} with a frequency stability of 0.007 cm^{-1}. Likewise, the dotted line in Fig. 6 represents the calculated optical depth, $\bar{\tau}_0$, for a Raman shifted dye laser having a linewidth of about 0.03 cm^{-1} and a frequency stability of 0.007 cm^{-1}. With the appropriate spectral weighting, then, the experimental data and calculations agree, which indicates a high spectral purity for both the laser and the Raman-shifted radiation, and thus the feasibility of using the SRS radiation for DIAL measurements.

VI. CONCLUSION

In summary, we have shown that stimulated Raman scattering of dye laser radiation is an efficient method for generating intense radiation at 765 and at 940 nm. In addition, the narrow bandwidth of the dye laser output was shown to be preserved in the scattering process for hydrogen pressures up to 14 atm, indicating that the tunable, infra-red radiation needed for DIAL measurements can certainly be generated in this manner.

11

Using a 2 m focal length lens to focus the pump radiation at the center of a Raman cell containing 14 atm of hydrogen, we measured a first Stokes energy conversion efficiency of 45% and 37% at 765 and 940 nm, respectively. For this geometry, there was negligible second Stokes light present, and the efficiency for generating first Stokes radiation in the backward direction was less than 1%. Higher conversion efficiencies were recorded as the pressure was increased to 28 atm, reaching 52% and 42% at 765 and at 940 nm respectively, but with a linewidth greater than 0.05 cm^{-1} which is too broad for most atmospheric DIAL applications.

In order to optimize the first Stokes generation at a given pressure of hydrogen, we needed to ensure that the pump angles did not extend so far as to encompass the phase matching angle for gain suppression to occur. We needed to reduce or eliminate the generation of first Stokes in the backward direction as well as the generation of higher order Stokes and anti-Stokes orders. The first Stokes radiation generated in the backward direction increases strongly as the pump confocal beam parameter is reduced. In addition, the generation of second Stokes light, by four-wave mixing of the original pump and the generated first Stokes, is reduced by using as collimated a pumping geometry as possible since then the beams are contained within angles less than the phase matching angle for the four-wave mixing process. Since the phase matching angle varies as the square root of the pressure, the angular requirements are quite stringent in the present narrow linewidth application where low pressures are a necessity. All of these considerations indicate that maximum energy can be extracted at the first Stokes frequency by using a pump geometry with as large a confocal beam parameter as possible for the cell length used.

The absorption measurements made in the oxygen A-band demonstrate the high spectral purity of the dye laser and, moreover, confirm that the Raman scattering process is capable of retaining the spectral purity of the pump radiation up to pressures capable of sustaining energy conversion levels of about 40%. The optical depth measurements at the line centers of 25 transitions in the oxygen A-band establish that Raman-shifted tunable dye laser radiation can be used for quantitative meteorological lidar measurements. The efficient generation of radiation at 940 nm is significant for lidar measurements of stratospheric water vapor. Also, by changing the pump wavelength to 773 nm, the first Stokes radiation at 1140 nm would allow coverage of the next water vapor band which has lines with strengths twice those found in the 940 nm band system. Solid state lasers such as alexandrite, which is tunable from 720 to 780 nm,[18] and Ti:sapphire, which is tunable from 700 to 920 nm,[22] could be used as pumps for generating near infrared radiation out to 1500 nm using stimulated Raman scattering in hydrogen. Further work is in progress to demonstrate the use of Raman scattered radiation in measurements of water vapor in the near infrared bands.

REFERENCES

1. E.V. Browell, T.D. Wilkerson and T.J. McIlrath, "Water Vapor Differential Absorption Lidar Development and Evaluation, "Appl. Opt. **18**, 3474 (1979).

2. C. Cahen, G. Megie and P. Flamant, "Lidar Monitoring of the Water Vaopr Cycle in the Troposphere," J. Appl. Meteorol. **21**, 2506 (1982).

3. E.V. Browell, A.K. Goroch, T.D. Wilkerson, S. Ismail, and R. Markson, "Airborne DIAL Water Vapor Measurements over the Gulf Stream," Proc. Twelfth International Laser Radar Conf., Aix en Provence, 151 (Etablissement d'Etude et de Recherche Meteorologique, Paris, 1984).

4. T.D. Wilkerson and G.K. Schwemmer, "Lidar Techniques for Humidity and Temperature Measurement," Opt. Eng. **21**, 1022 (1982).

5. C.L. Korb and C.Y. Weng, "A Theoretical Study of a Two-Wavelength Lidar Technique for the Measurement of atmospheric Temperature Profiles," J. Appl. Meteorl. **21**, 1346 (1982).

6. C.L. Korb and C.Y. Weng, "Differential Absorption Lidar Technique for Measurement of the Atmospheric Pressure Profile," Appl. Opt., **22**, 3759 (1983).

7. T.D. Wilkerson, G.K. Schwemmer, L.J. Cotnoir, and U.N. Singh, "On the Measurement of Atmospheric Density Using DIAL in the O_2 A-Band (770 nm)," Proc. 13th Internat. Laser Radar conf., Toranto, Canada. NASA Conf. Publ. 2431 (1986).

8. T.D. Wilkerson, G.K. Schwemmer, K.J. Ritter, U.N. Singh, and R. Mahon, "Applications of Laser and LIDAR Spectroscopy to Meteorological Remote Sensing," Laser Spectroscopy VIII (eds. W. Persson and S. Svanberg), Springer-Verlag, New York (1987).

9. L.P. Giver, B. Gentry, G. Schwemmer, and T.D. Wilkerson, "Water Absorption Lines 931-961 nm: Selected Intensities, N_2 Collision broadening Coefficients, Self-Broadening Coefficients, and Pressure Shift in Air," J. Quant. Spectrosc. Radiat. Transfer 27, 423 (1982).

10. E.V. Browell and S. Ismail, "Spaceborne Lidar Investigations of the Atmosphere," Proc. ESA Workshop on Space Laser Applications and Technology, Les Diablerets, Switzerland (1984).

11. C. Cahen and G. Megie, "A Spectral Limitation in the Range Resolved Differential Absorption Lidar Technique," J. Quant. Spectros. Radiat. Transfer 25, 151 (1981).

12. J.R. Murray and A. Javan, "Effects of Collisions on Raman Line Profiles of Hydrogen and Deuterium Gas," J. Mol. Spectrosc. 42, 1 (1972).

13. W.H. Lowdermilk and G.I. Kachen, "Spatial and Temporal Intensity Distribution of Stimulated Raman Emission," J. Appl. Phys. 50, 3871 (1979).

14. B.E. Grossmann, U.N. Singh, N.S. Higdon, L.J. Cotnoir, T.D. Wilkerson, and E.V. Browell, "Raman-Shifted Dye Laser for Water Vapor DIAL Measurements,"Appl. Optics, 26, 1617 (1987).

15. U.N. Singh, Z. Chu, R. Mahon, and T.D. Wilkerson, "Optimization of a Raman-Shifted Dye Laser System for DIAL Applications," Proc. 14th Internat. Laser Radar Conf. San Candido, Italy (1988).

16. B.N. Perry, P. Robinowitz and D.S. Bomse, "Stimulated Raman Scattering with a Tightly Focussed Pump," Opt. Lett., 10, 146 (1985).

17. E.W. Washburn, ed., International Critical Tables of Numerical Data (McGraw-Hill, New York), 7, 11 (1930).

18. G.K. Schwemmer, M. Dombrowski, C.L. Korb, J. Milrod, H. Walden, and R.

Kagann, "A Lidar System for Measuring Atmospheric Pressure and Temperature Profiles," Rev. of Scient. Instr. **58**, 2226 (1987).

19. K.J. Ritter, "A High Resolution Spectroscopic Study of Absorption Line Profiles in the A-Band of Molecular Oxygen" Ph.D dissertation, University of Maryland (1986).

20. L. J. Cotnoir, J. A. McKay and P. M. Laufer, "Integrated Spectrum Analyzer/Wavemeter for Pulsed, Tunable Lasers," *SPIE Proc. 889, Airborne & Spaceborne Lasers for Terrestrial Geophysical Sensing*, F. Allario, Editor (1988).

21. K.J. Ritter and T.D. Wilkerson, "High Resolution Spectroscopy of the Oxygen A-Band," J. of Mol. Spectrosc. **121**, 1 (1987).

22. P. Brockman, C.H. Bair, J.C. Barnes, R.V. Hess, and E.V. Browell, "Pulsed Injection Control of a Titanium-Doped Sapphire Laser," Opt. Lett. **11**, 712 (1986).

FIGURE CAPTIONS

Fig. 1. Schematic diagram of the experiment for generating the first Stokes at 765 nm using a dye laser pump at 580 nm. The first Stokes at 940 nm was generated in like manner from a 676 nm pump using appropriate dichroics. The multi-pass White cell is indicated, and A and B designate the pyroelectric energy probes used to ratio the transmitted to incident energies.

Fig.2. Energy conversion efficiency as a function of pressure when generating the first Stokes at 765 nm in (a) and at 940 nm in (b). The pump beam was focussed into the center of the Raman cell with lenses having focal lengths of: 2 m; 1.5 m; 1 m; and 0.5 m. A constant pump energy of 29 mJ at 580 nm was used in (a) while a pump energy of 25 mJ at 676 nm was used in (b).

Fig. 3. First Stokes energies at both 765 nm and at 940 nm as a function of pump energy for two pump geometries and a hydrogen cell pressure of 14 atm.
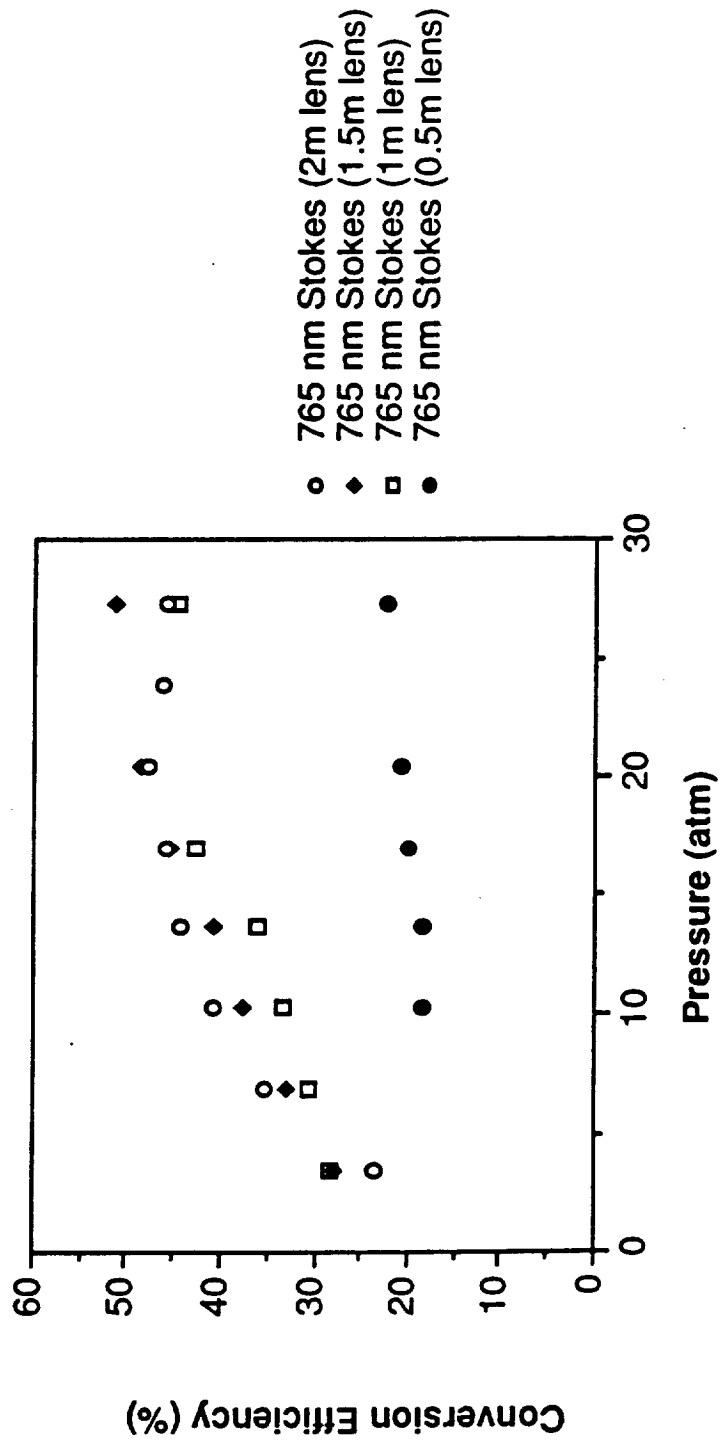
Fig. 4. Conversion efficiency for the 940 nm first Stokes radiation generated in the backward direction as a function of hydrogen pressure for two pump geometries.
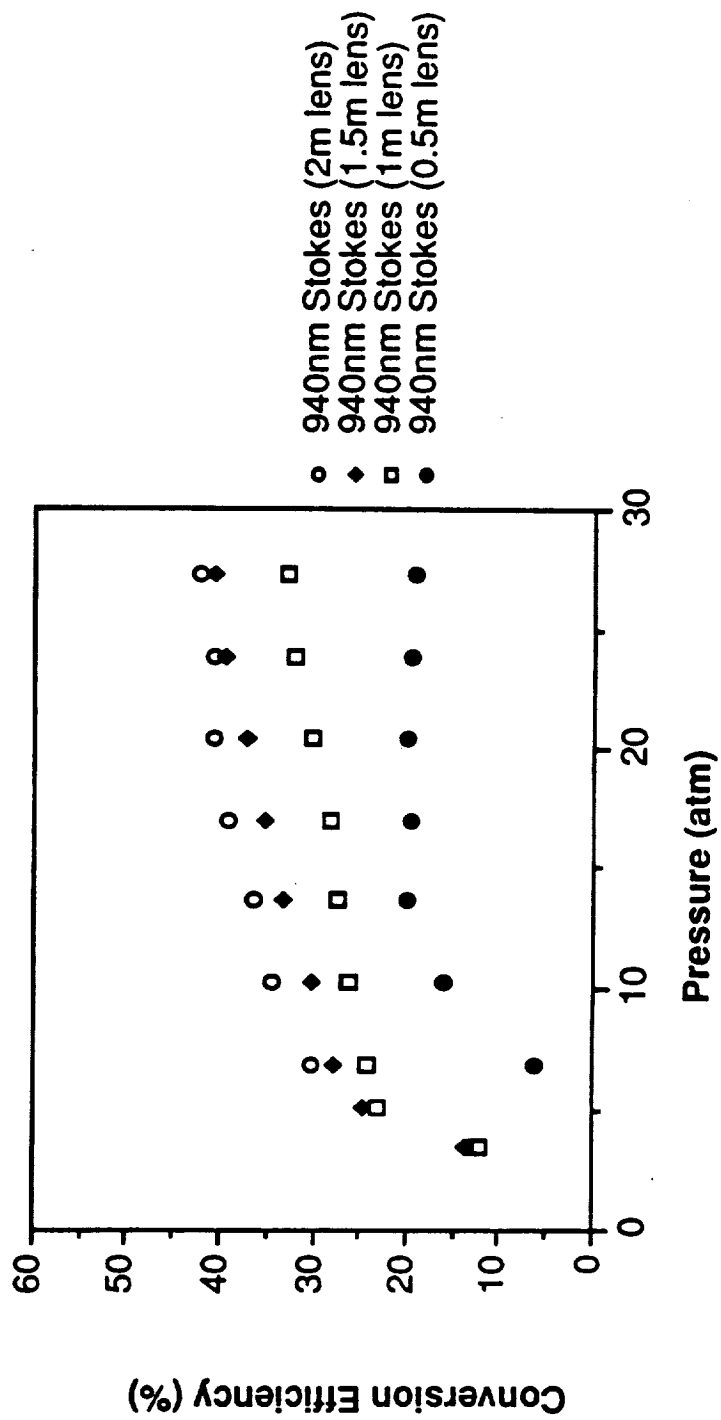
Fig. 5. Optical depths of lines in the A-band of molecular oxygen, as measured using the 760-770 nm dye laser radiation, compared with the

17

calculated optical depth for the dye laser linewidth of 0.02 cm^{-1} with a frequency stability of 0.007 cm^{-1}.
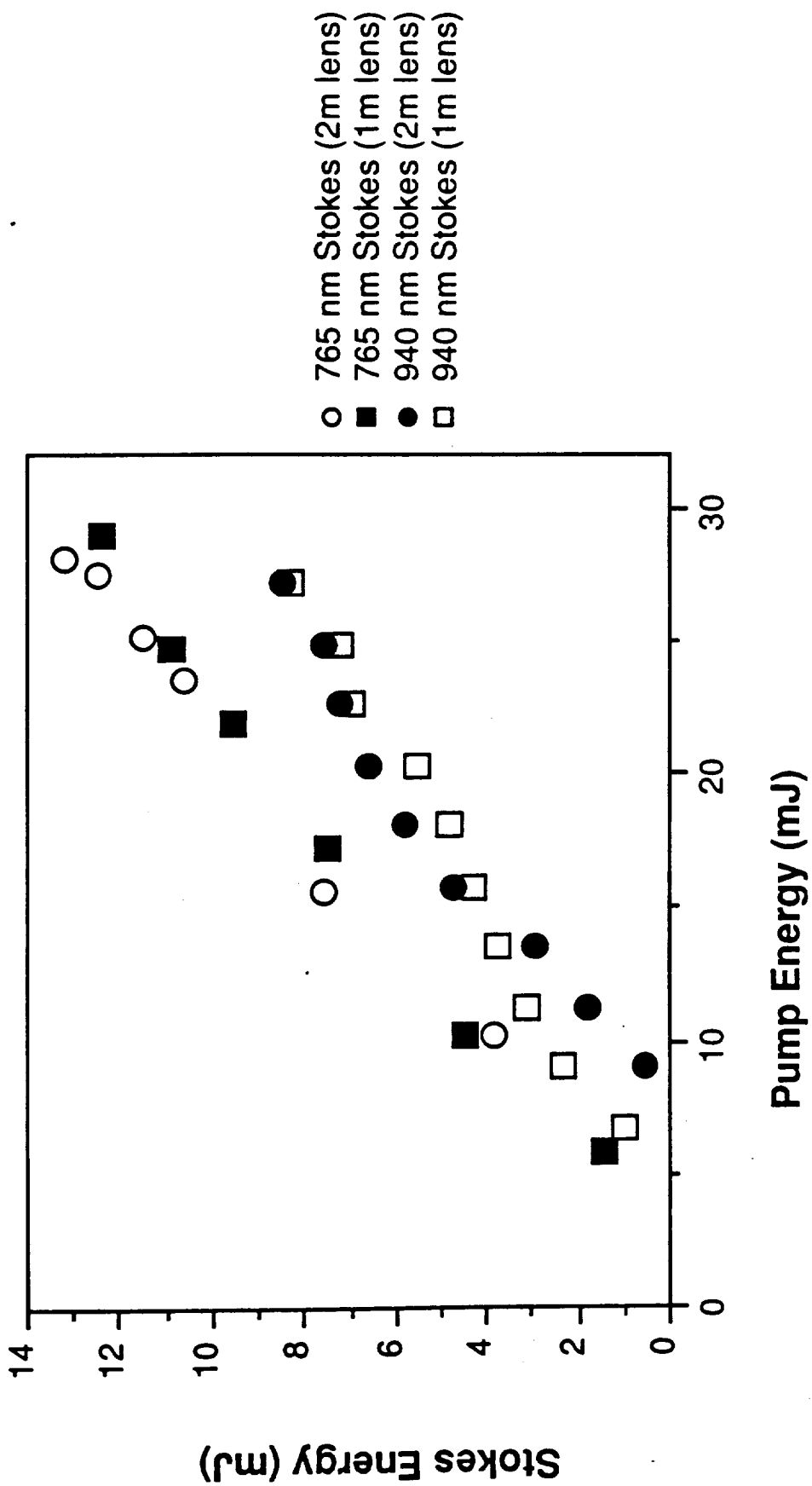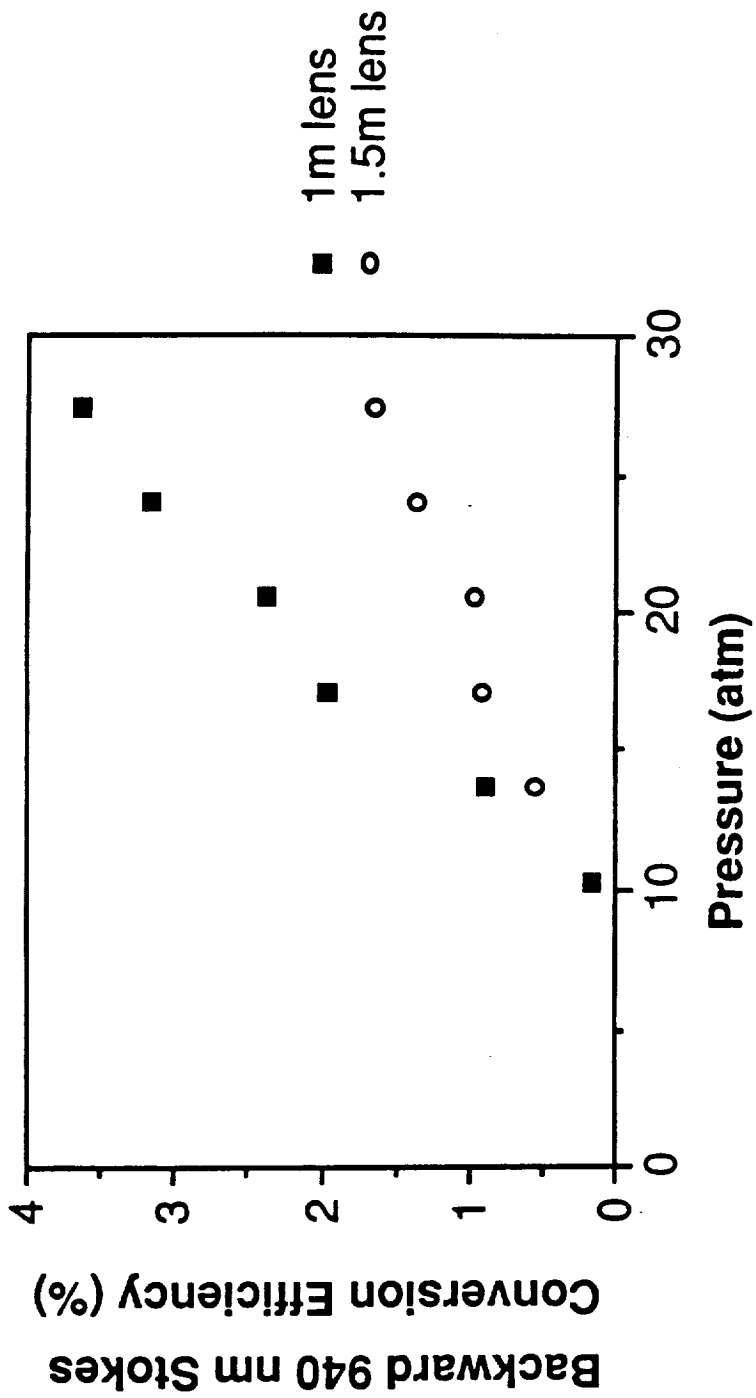
Fig. 6. Optical depths of lines in the A-band of molecular oxygen, as measured using the 760-770 nm Raman-shifted dye laser radiation, compared with the calculated optical depth for the dye laser linewidth of 0.03 cm^{-1} with a frequency stability of 0.007 cm^{-1}.

Raman Cell

765nm
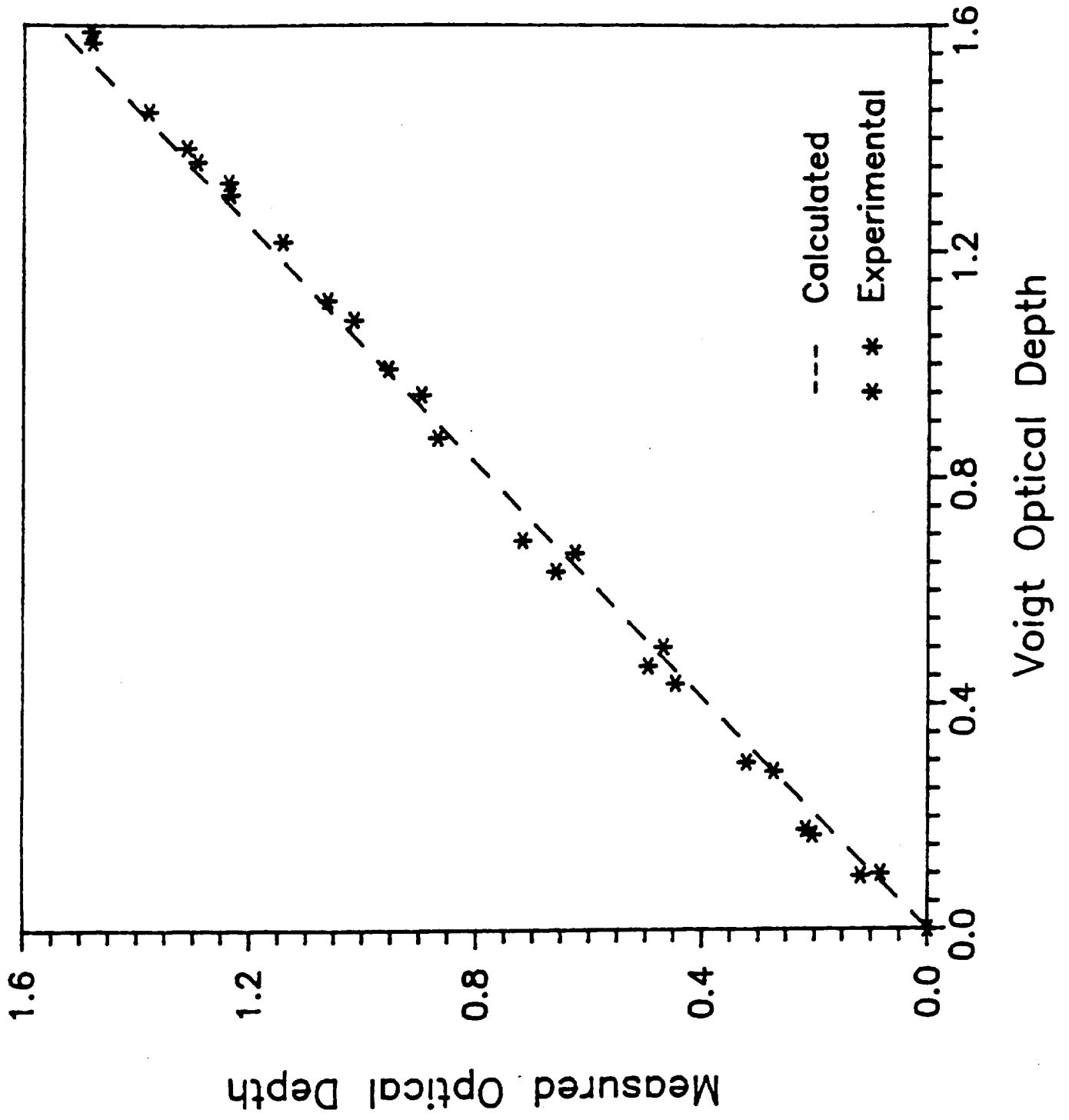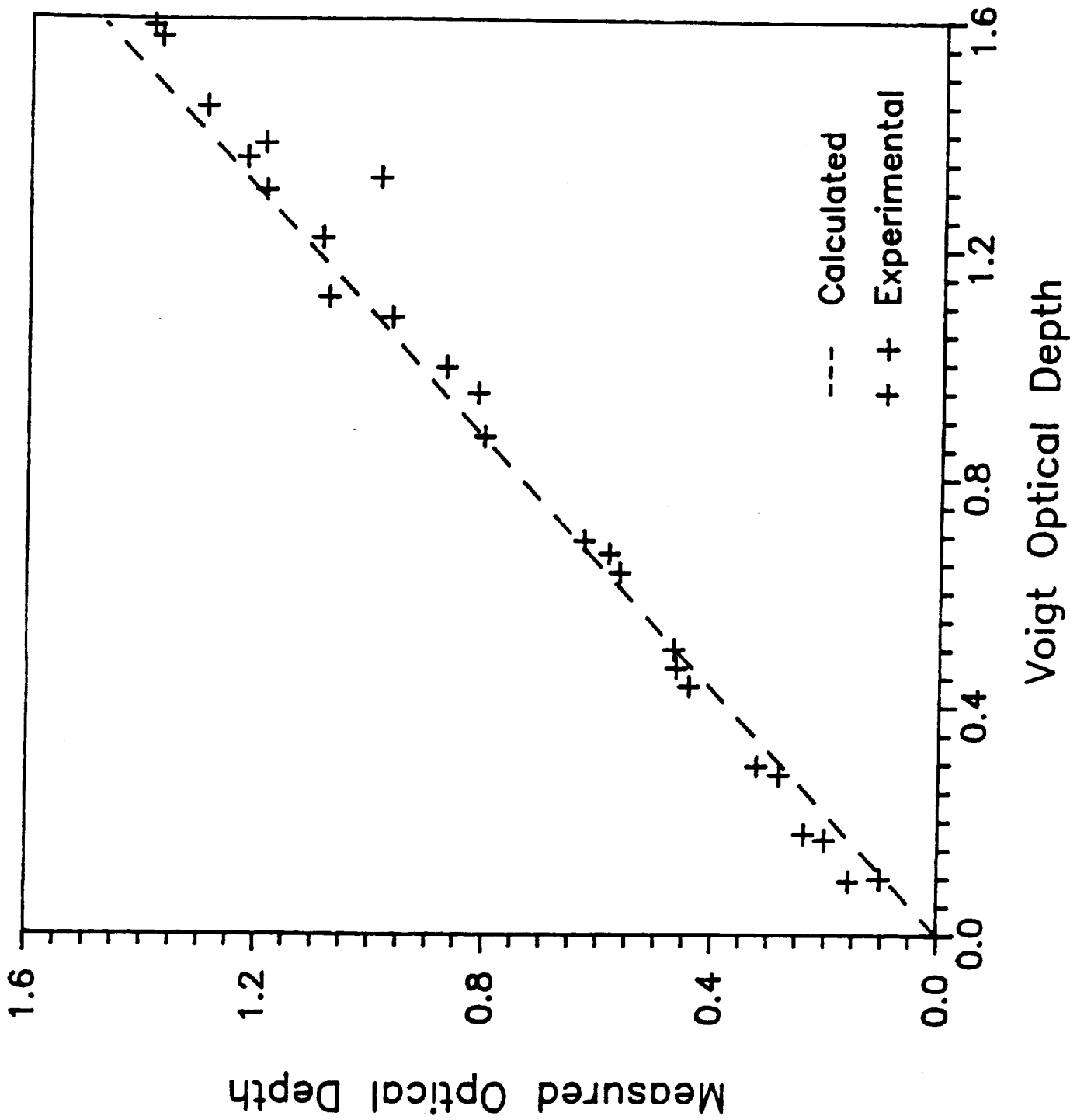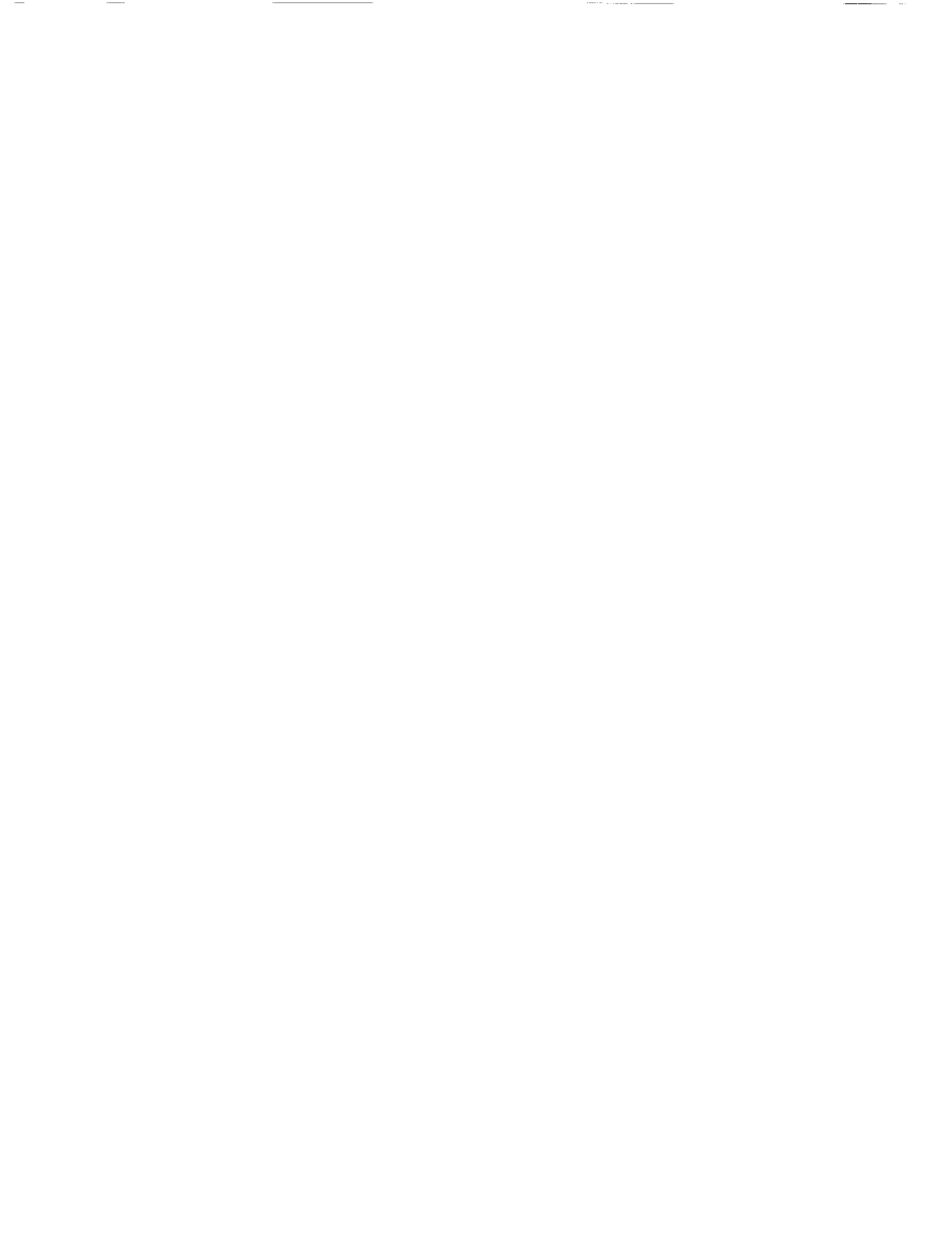
580nm

Fabry Perot Interferometer

White Cell

A

B

OMA

580nm/765nm

Dye Laser

Amp

Pre Amp

Osc

532nm

Wave Meter

Frequency Doubled Nd:YAG LASER

765 nm Stokes (2m lens)
765 nm Stokes (1.5m lens)
765 nm Stokes (1m lens)
765 nm Stokes (0.5m lens)

Pressure (atm)

Conversion Efficiency (%)

Conversion Efficiency (%)

Pressure (atm)

○ 940nm Stokes (2m lens)
◆ 940nm Stokes (1.5m lens)
□ 940nm Stokes (1m lens)
● 940nm Stokes (0.5m lens)

Fig. 3

ingh, Chu, Mahon & Wilkerson

Backward 940 nm Stokes Conversion Efficiency (%)

Pressure (atm)

■ 1m lens
○ 1.5m lens

Singh, Chu, Mahon & Wilkerson

Fig 4

Voigt Optical Depth

Measured Optical Depth

- - - Calculated
* * Experimental

Voigt Optical Depth

Measured Optical Depth

--- Calculated
+ + Experimental

APPENDIX C

A SELF-SEEDED SRS SYSTEM FOR THE GENERATION
OF 1.54 μm EYE-SAFE RADIATION

Z. CHU, U. N. SINGH, and T. D. WILKERSON

University of Maryland

Institute for Physical Science and Technology

College Park, MD 20742-2431

Abstract

We report experiments on the generation of infrared radiationat 1.54 μm by means of stimulated Raman scattering in CH_4 gas pumped by a Nd:YAG laser at 1.06 μm. A compact, self-seeded system using the backward first Stokes radiation as the seed has been developed to improve the forward first Stokes conversion efficiency. Output pulse energy of 25 mJ at 1.54 μm is obtained for a pump energy of 140 mJ at 10 Hz, and the beam divergence is measured to be less than 1 mrad. The first Stokes conversion efficiency and the spatial beam quality of the output were found to depend strongly on the pump laser repetition rate. Higher pump repetition rate creates a thermal gradient at the interaction region affecting the conversion efficiency and spatial beam quality adversely. The optimized results demonstrate the applicability of this radiation for eye-safe lidar measurements.

1. Introduction

The most commonly used LIDAR (light detection and ranging) systems are not eye-safe and pose potential risk of eye damage especially in the case of downward pointing airborne lidar systems. Laser radiation of wavelength greater than 1.4 μm is considered eye-safe at least as regards to retinal damage. A short wavelength lidar capable of operating in nominally eye-safe spectral regions is needed for cloud and aerosol studies [1,2]. A Raman-shifted Nd:YAG laser capable of generating 1.54 μm radiation can be developed to qualify as an eye-safe lidar [3,4]. The eye-safety criterion set by the American National Standard Institute (ANSI) for a single pulse exposure is: 1 J/cm^2 at 1.54 μm, which is specified to be about 400,000 times safer, for eye exposure, than the Nd:YAG laser (1.06 μm) [3].

Stimulated Raman scattering (SRS) has been widely used to generate laser wavelengths in spectral regions where conventional laser sources are not available. This is one of the most efficient methods for frequency-shifting radiation from the visible or near-infrared to the infrared. The technique is attractive because of its simplicity and its low activation threshold, which is readily reached with conventional lasers. Light at 1.54 μm wavelength can be generated as first Stokes radiation by passing 1.064 μm radiation, from a Nd:YAG laser, through compressed methane. Optimization techniques are very useful for increasing SRS conversion efficiency in the infrared because the Raman gain decreases with increasing wavelength.

In this paper, we report results of a study of SRS in CH_4 using 1.06 μm pump radiation and employing a backward Stokes seeding scheme in a single pass Raman cell. We also describe the different experimental optimization techniques employed and advantages of backward Stokes seeded SRS. We point out advantages and difficulties encountered in using CH_4 as a Raman shifting

gas, and discuss several solutions and recommendations about this SRS technique.

2. Experimental arrangement

The experimental arrangement is indicated in fig.1. The pump laser is a Nd:YAG laser (Quantel YAG 581-10) which generates randomly polarized radiation at 1.06 μm with pulse width of 10 ns and beam diameter of 0.6 cm. The pump beam was focused by lens L_1 at the middle of a 1 meter long Raman cell containing methane gas. The 45° dichroic mirror M_1 was highly transparent to 1.06 μm and reflective at 1.54 μm, and used for separating the backward Stokes seed from the pump radiation and for monitoring the energy of the pump pulse. The first Stokes radiation at 1.54 μm was generated in both forward and backward directions. The forward first Stokes light was collimated by L_3, separated by the 45° dichroic mirror M_3 (identical to M_1) and colored glass filters, and measured by a pyroelectric detector. In absence of any injection seeding, this configuration constituted a single-pass, self-generated SRS system.

The injection seeding was achieved by means of dichroic mirror M_1 (λ_{Rmax}=1.54 μm / λ_{Tmax}=1.06 μm, θ=45°), lens L_2 (focal length 50 cm), and dichroic mirror M_2 (λ_{Rmax}=1.54 μm / λ_{Tmax}=1.06 μm, θ=0°). The backward first Stokes light was used as a "seed" and separated from the pump beam by M_1. The beamsplitter BS was used for monitoring the seed pulse energy. The dichroic mirror M_2 was placed at 75 cm from the center of the Raman cell. The seed beam became collimated when it first passed through L_2; then it was reflected back by M_2 and refocused into the Raman cell by L_2. This injected seed was amplified by the rest of the pump pulse in the same cell. In this configuration, the Raman cell acts as an amplifier.

For a SRS amplifier, there are two important factors directly related to the amplifying efficiency: the temporal and spatial overlaps between the seed and pump waves. The temporal overlap between the seed and pump can be estimated by assuming that the backward first Stokes is generated at the focus of the pump radiation during the first pass through the Raman cell. The time delay T of the seed relative to the pump is T=2L/c, where L is the distance between the dichroic mirror M_2 and the focus of the pump beam, and c is the speed of the light. The temporal overlap may be maximized by minimizing L. Unfortunately L cannot be zero and, at a minimum, is equal to half the cell length. In this experiment, T turned out to be about 5 ns, which is half of the pump laser pulse width. Separating seed from pump increased the delay time but provided the advantage of focusing the pump and seed beams independently, and consequently obtaining a good spatial overlap between them for increased amplifying efficiency. The other advantage of this configuration, which was important for maximizing the first Stokes conversion efficiency, was the ease with which the spatial overlap between the pump and seed can be established by means of the two alignment mirrors (M_1 & M_2) in the seed line. For a fixed temporal overlap, the best alignment of the spatial overlap was judged by monitoring the spatial beam quality and energy of the net forward first Stokes radiation at 1.54 μm.

3. Experimental results and discussion

Readings were recorded from three energy meters monitoring the pump energy, the backward first Stokes (seed) energy and the amplified, injection-seeded forward first Stokes energy. For optimization of the first Stokes conversion efficiency, lenses of different focal length (50, 75, 100, 150, and 200 cm) were tried at different cell pressures of CH_4. The results

indicate that focusing the pump energy with a 100 cm focal length lens provides the optimum conversion efficiency and reasonable beam quality. We also attempted to use a beam reduction telescope (2x, 2.5x, 3x, and 3.5x) to increase the confocal parameter by sending a uniformly focused beam in the Raman cell. In all cases the pump levels were either below or barely above the threshold for first Stokes generation. Thus all the subsequent studies and optimization were conducted using a 100 cm focal length lens to focus the main pump beam in the Raman cell. The results are summarized in fig.2 through fig.5.

Fig.2 shows the conversion efficiencies of the pump laser to a) the backward first Stokes seed wave, and b) the injection-seeded forward first Stokes wave for different cell pressures. All the data were corrected for losses in the optics. It can be seen that the threshold pump energy for injection-seeded, forward first Stokes is lower than the backward first Stokes; for example, at 14 atm the threshold pump energy for the forward and backward cases is 84 and 112 mJ, respectively. As soon as the pump laser energy exceeded the thresholds, both backward Stokes seed and injection-seeded forward first Stokes rose rapidly and reached the maximum of 2% and 18%, respectively, for a pump energy of 126 mJ. When the pump energy was increased further, the forward Stokes conversion efficiency attained saturation while the backward Stokes seed slowly dropped. With 140 mJ pump energy, the backward Stokes efficiency dropped to 1.6% but forward Stokes efficiency remained at 18%.

The pressure dependence of the SRS gain in compressed methane in the forward direction can be written as [5,6]

$$g_s = k \, P \, / \, (\, 0.32 + 0.012 \, P \,) \qquad (1)$$

where k is a constant, and P is the pressure in atm. The gain coefficient,

5

when calculated with eq.(1), indicates that in the pressure range 0 - 25 atm, g_s does not deviate much from the linear range; this agrees with the previous measurement [7]. Figure 3 explicitly indicates the pressure dependence of the injection-seeded first Stokes conversion efficiency, as observed in our experiment. For a pump energy above 112 mJ, the conversion efficiency reaches saturation at a pressure around 14 atm. This downward shift of saturation pressure, as the pump energy is increased, could be caused by higher order Stokes generation or by some other competing nonlinear processes in the Raman cell. This would lead to pump depletion at higher pressure and limit the SRS conversion efficiency.

Second Stokes generation in the forward direction is possibly the main reason for the phenomenon of the down shift of the pressure saturation observed in our experiment and depicted in Fig.3. The second Stokes light is generated either by four wave mixing of the pump, first Stokes, and first anti-Stokes radiation, or by the Raman cascade effect when the first Stokes radiation is strong enough to drive the second Stokes process. The build-up of second Stokes intensity will decrease the first Stokes field no matter how it originates. Unfortunately, we could not make a quantitative measurement of the second Stokes intensity because the output windows of the Raman cell were made of fused silica or BK7, both of which materials have transmission of less than 5% at the second Stokes wavelength of 2.8 μm. For the pump energy levels used in our experiment, the generation of the third and other higher order Stokes can be considered negligible [8].

In our experiment, stimulated Brillouin scattering (SBS) was observed to be one of the nonlinear processes competing with the SRS in compressed methane. At 140 mJ of pump energy and 20 atm pressure, 7% of the pump energy was converted to the backward SBS component and was found to increase with

pressure. This depletion in pump energy due to SBS could possibly explain the drop in the first Stokes conversion efficiency, as shown in fig 2(b), when the CH_4 pressure was increased from 14 to 20 and 34 atm.

A process that, in effect limits the SRS conversion efficiency is gas breakdown. When high energy pump pulses were focused tightly using a short focal length lens (e.g.,50 cm) at 10 Hz repetition rate, the power at the focal point in the Raman cell exceeded the breakdown threshold of methane. Solid carbon particles were generated in the gas breakdown. These particles were found sticking to the inside window surface occasionally and would burn when hit by the laser beam, causing severe damage to the inside surface of the coated window. The multiple burn inhibited further operation and resulted in decreased conversion efficiency and degraded output beam quality. To circumvent this problem we constrained ourselves to use only uncoated windows, to avoid tight focusing by using longer focal length lenses, and to employ moderate pump energy levels.

Measurements were undertaken to demonstrate the advantage of injection seeding over the unseeded SRS process. The unseeded forward first Stokes conversion efficiency was measured simply by blocking the M2 mirror. In the injection-seeded case we also simultaneously monitored the backward first Stokes seed energy through the beamsplitter BS. The results are shown in fig. 4, where the backward first Stokes seed, unseeded and injection-seeded forward first Stokes conversion efficiency is plotted as a function of pump energy for a cell pressure of 14 atm. The injection seeding results in lower threshold for Stokes generation; and for a pump energy above threshold the efficiency increases considerably. For a pump energy of 140 mJ, the injection-seeded forward first Stokes efficiency reaches three times than the unseeded Stokes efficiency, with an output energy of 25 mJ. The spatial beam

concave moon. It was found during the experiment that the half moon diameter was proportional to the laser repetition rate, the pump energy and the gas pressure. The beam quality improved considerably at the lower laser repetition rate. At 3 Hz the half moon was almost flat at the top. This improvement in the laser beam quality and higher first Stokes energy at the lower laser repetition rate indicates that a thermal gradient, is established at the interaction region at higher repetition rate, with not enough time between the successive pulses to dissipate the heat, thus resulting in a beam blow-up and lower conversion efficiency. Work is in progress for developing techniques to dissipate the heat between the successive pulses, and thus to operate the Raman cell possibly at 50 Hz for improved lidar data acquisition and better signal-to-noise ratio.

Studies were also conducted to estimate the divergence of the first Stokes output at 1.54 μm. Initial measurements indicated that by operating at a cell pressure of 14 atm and using a lens of focal length of 100 cm to focus the pump beam and a lens of focal length 75 cm to collimate the forward Stokes beam, the divergence of injection-seeded first Stokes beam was around 1 mrad, which happens to be well suited for the lidar measurements intended. Detail studies using distant solid target are needed for establishing exact divergence.

4. Conclusions

We have investigated the performance of a self-injection-seeded SRS system, using methane gas as the Raman medium, and have optimized the SRS conversion to the first Stokes radiation at 1.54 μm. Compared to the single pass self-generated SRS system, the conversion efficiency tripled and approached 18% at a pressure of 14 atm and a pump energy of 140 mJ at 10 Hz.

PRECEDING PAGE BLANK NOT FILMED

The conversion efficiency is further improved by operating the system at lower repetition rate (e.g., 5 or 3 Hz). The enhanced conversion efficiency supports the feasibility of using 1.54 μm eye-safe radiation for multiwavelength lidar measurements. Further work is in progress to run the system at higher repetition frequency with enhanced conversion efficiency.

Acknowledgements

References

[1] R. M. Measures, Laser remote sensing (John Wiley & Sons, New York, 1984).

[2] E.M.Patterson, D.W. Roberts, G.G. Gimmestad, Conf. on Laser and Electrooptics, Baltimore, Maryland, April 1989, paper PD 26

[3] J.T. Lin, Proc. of Intern. Conf. on Laser 1986, Orlando, Florida, November 1986.

[4] C.G. Parazzoli, W.W. Buchman, R.D. Stultz, IEEE J. Quantum. Electron. QE-24 (1988) 872.

[5] Y. Taira, K. Ide and H. Takuma, Chem. Phys. Lett 91 (1982) 299.

[6] J.R. Murray, J. Goldhar, and A. Szöke, Appl. Phys. Lett. 32 (1978) 551.

[7] R.W. Minck, E.E. Hagenlocker, and W. G. Rado, J. Appl. Phys. 38 (1967) 2254.

[8] C. Guntermann, V.S. Gatten, and H.F. Dobele, Applied Optics, 28 (1989) 135.

FIGURE CAPTIONS

Fig. 1. Experimental setup.

Fig. 2. Energy conversion efficiency as a function of pump energy to (a) the backward first Stokes seed, and (b) the injection-seeded forward first Stokes for different gas pressures: □ , 10 atm; ● , 14 atm; Δ , 20 atm; O , 34 atm.

Fig. 3. Conversion efficiency to the injection-seeded first Stokes as a function of gas pressure for different pump energy: ● , 140 mJ; □ , 112 mJ; ▲ , 84 mJ; O , 70 mJ.

Fig. 4. Conversion efficiency for the injection-seeded first Stokes (●) as a function of pump energy for a gas pressure of 14 atm. As a comparison, the conversion efficiency for the backward first Stokes seed (o) and the forward first Stokes in the unseeded case(■) are also shown.

Fig. 5. Conversion efficiency for the injection-seeded first Stokes as a function of pump energy for two different focusing geometries and gas pressures: □ , 14 atm & F_{L1}= 1 m; O , 14 atm & F_{L1}= 0.75 m; ■ , 34 atm & F_{L1}= 1 m; ● , 34 atm & F_{L1}= 0.75 m.

Figure 1.

Figure 2.

Figure 3.

Chu, Singh & Wilkerson

Figure 4.

Conversion Efficiency (%)

Pump Energy (mJ)

Chu, Singh & Wilkerson
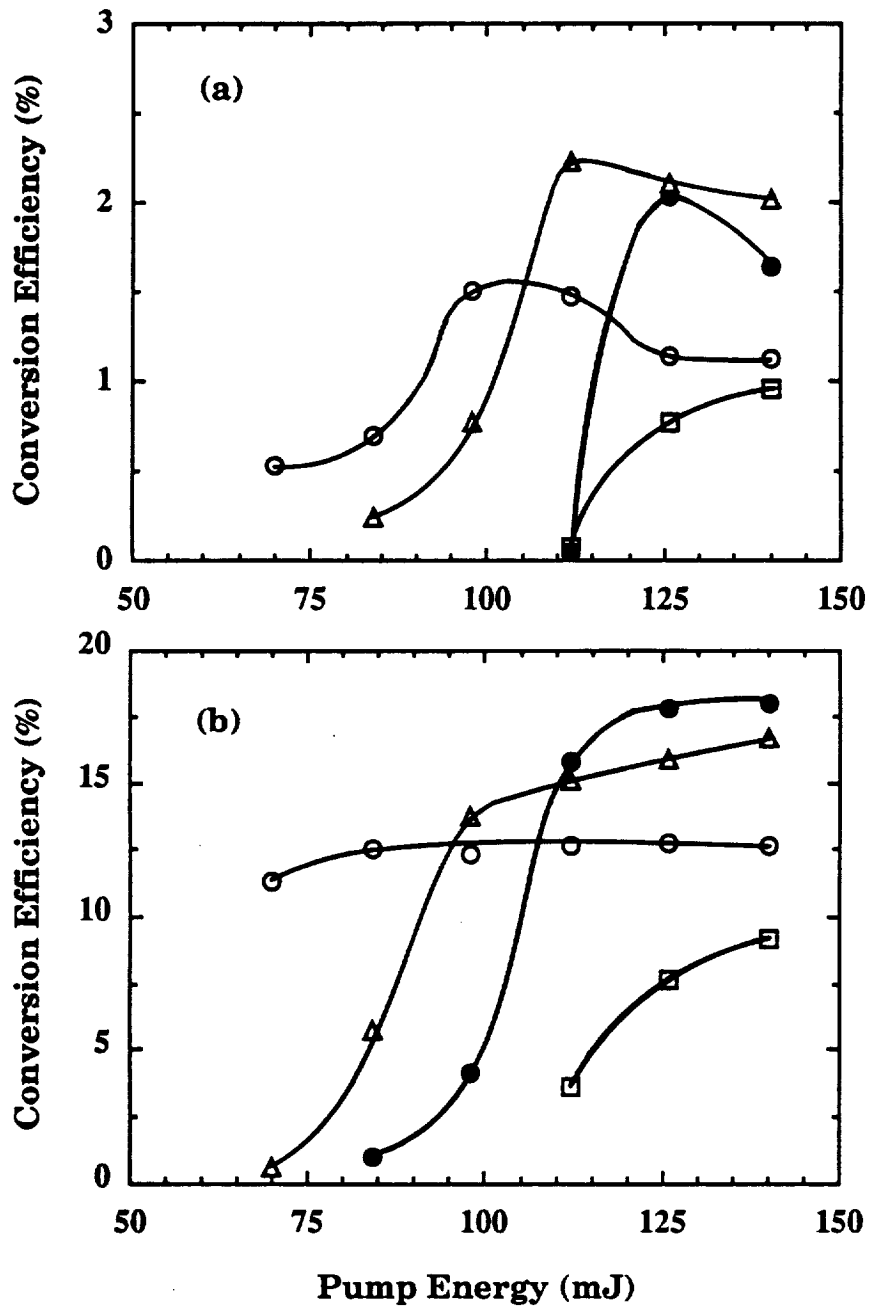
Figure 5.

Conversion Efficiency (%)

Pump Energy (mJ)

Chu, Singh & Wilkerson
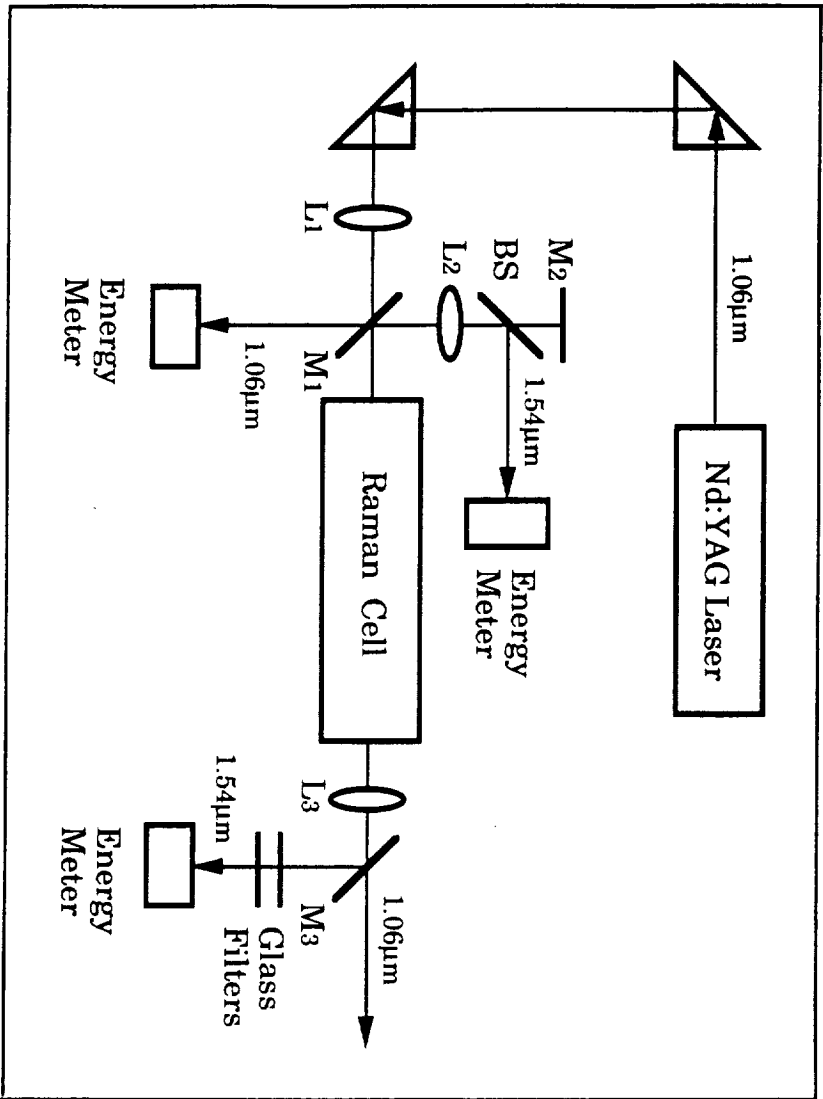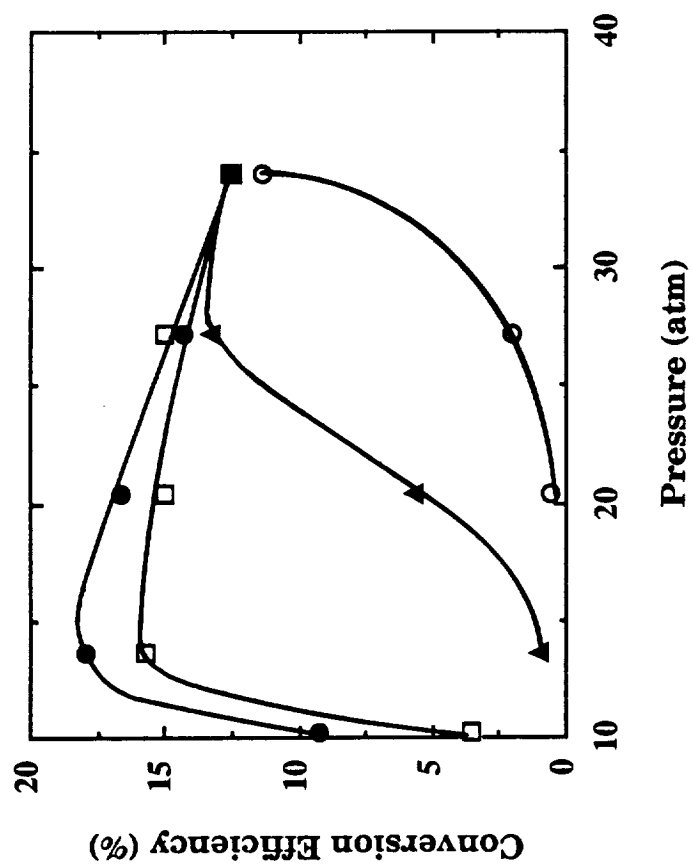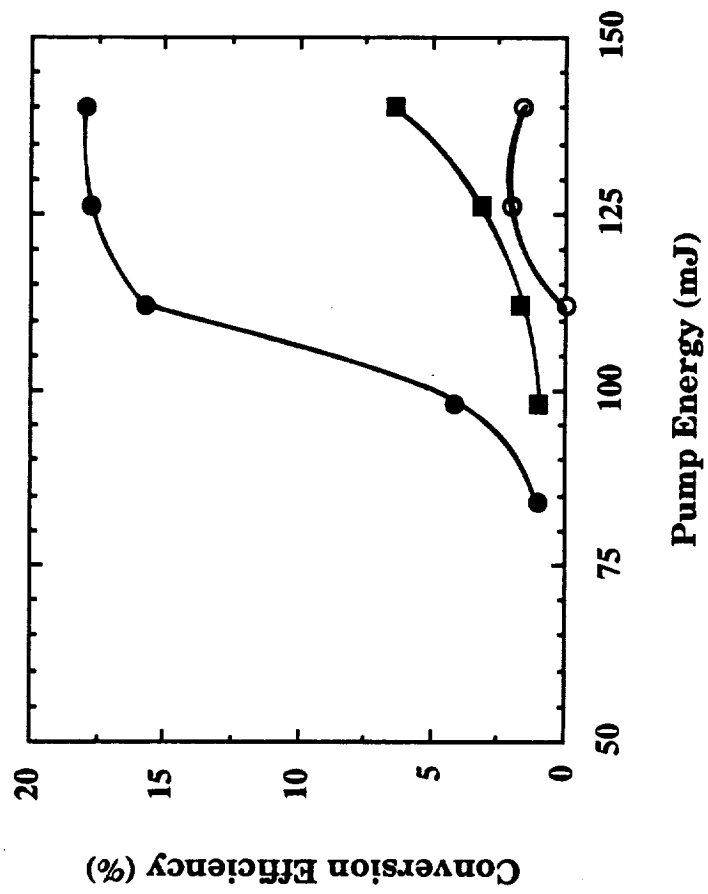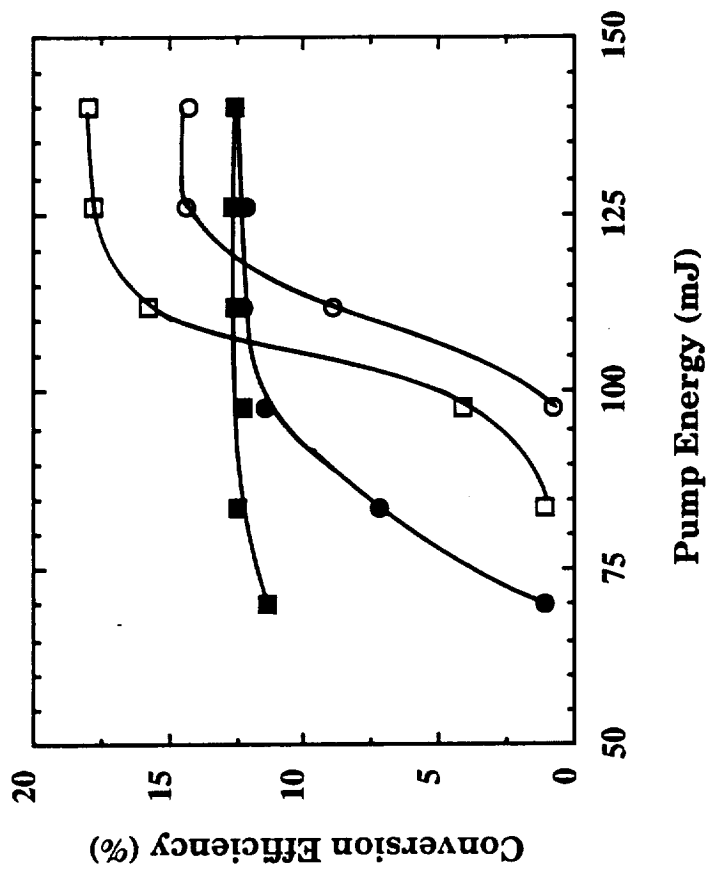
APPENDIX D

EFFICIENT NEAR-IR LIGHT SOURCE FOR

EYE-SAFE LIDAR APPLICATIONS

U. N. SINGH, Z.CHU, and T. D. WILKERSON

Atmospheric Lidar Observatory
Institute for Physical Science and Technology
University of Maryland
College Park, MD 20742-2431

Abstract

A light source for efficient, 1.54 μm eyesafe aerosol lidar operation is described, using Nd:YAG output (1.06 μm) Raman-shifted (amplified) in methane.

1

EFFICIENT NEAR-IR LIGHT SOURCE FOR
EYE-SAFE LIDAR APPLICATIONS [1]

U. N. SINGH, Z.CHU, and T. D. WILKERSON

Atmospheric Lidar Observatory
Institute for Physical Science and Technology
University of Maryland
College Park, MD 20742-2431

The most commonly used lidar (light detection and ranging) systems are not eye-safe and pose potential risk of eye damage especially in the case of downward pointing airborne lidar systems. A short wavelength lidar capable of operating in nominally eye-safe spectral regions (1.54 μm) is needed for cloud and aerosol studies [2,3]. A Raman-shifted Nd:YAG laser capable of generating 1.54 μm radiation can be developed to qualify as an eye-safe lidar [4,5,6]. The eye-safety criterion set by the American National Standard Institute (ANSI) for a single pulse exposure is: 1 J/cm^2 at 1.54 μm, which is specified to be about 400,000 times safer, for eye exposure, than Nd:YAG laser radiation at 1.06 μm [4].

In this paper, we report results of a study of stimulated Raman scattering (SRS) in compressed methane using 1.06 μm as the pump radiation and employing a backward Stokes seeding scheme in a single pass Raman cell for improving the forward Stokes conversion efficiency at 1.54 μm. Optimization techniques and limitations involved are also described.

The experimental arrangement is indicated in Fig.1. The pump radiation at 1.06 μm has a pulse width of 10 ns, beam diameter of 0.6 cm and divergence of 0.6 mrad. The pump beam was focused by lens L_1 at the middle of a 1 meter long Raman cell containing methane gas. The first Stokes radiation at 1.54 μm was generated in both forward and backward directions. The injection seeding was achieved by means of dichroic mirror M_1 (λ_{Rmax}=1.54 μm / λ_{Tmax}=1.06 μm, θ=45°), lens L_2 (focal length 50 cm), and dichroic mirror M_2 (λ_{Rmax}=1.54 μm / λ_{Tmax}=1.06 μm, θ=0°). The backward first Stokes light was used as a "seed" and separated from the pump beam by M_1. The seed beam became collimated when it first passed through L_2; then it was reflected back by M_2 and refocused into the Raman cell by L_2.. This injected radiation was amplified by the rest of the pump pulse in the same cell. In this configuration, the Raman cell acts as an amplifier.

Readings were recorded from three energy meters monitoring the pump energy, the backward first Stokes (seed) energy and the amplified, injection-seeded forward first Stokes energy. For optimization of the first Stokes conversion efficiency, lenses of different focal length (50, 75, 100, 150, and 200 cm) were used at different cell pressures of CH_4. The results indicated that focusing the pump energy with a 100 cm focal length lens provides the optimum conversion efficiency and reasonable beam quality. The results are summarized in Fig.2 through Fig.4.

Figure 2 shows the conversion efficiencies of the pump laser to the injection-seeded forward first Stokes wave for different cell pressures. Figure 3 explicitly indicates the pressure dependence of the injection-seeded first Stokes conversion efficiency, as observed in our experiment. From these two results it can be easily seen that for a pump energy above 112 mJ, the conversion efficiency reaches saturation at a pressure around 14 atm. This downward shift of saturation pressure, as the pump energy is increased, may be caused by higher order Stokes generation or some other competing nonlinear processes in the Raman cell. This would lead to pump depletion at higher pressure and limit the SRS conversion efficiency.

Figure 4 shows the conversion efficiencies of the backward first Stokes, injection-seeded and unseeded forward first Stokes as a function of pump energy for a cell pressure of 14 atm. Advantages of injection seeding are quite evident. Injection seeding results in lower threshold for Stokes generation; and for a pump energy above threshold the efficiency increases considerably. For a pump energy of 140 mJ, the injection-seeded forward first Stokes efficiency reaches three times than the unseeded Stokes efficiency. The spatial beam quality of the seeded Stokes beam was also found to be much better than the unseeded Stokes beam.

We observed two limiting factors on the SRS conversion efficiency. One is gas breakdown, which occurs when high energy pump pulses are focussed by a short focal length lens (e.g., 50 cm.). Another is the repetition rate of the pump laser. The conversion efficiency increased considerably at lower repetition rate (5 and 3 Hz). The spatial beam quality of both the transmitted pump and the Stokes radiation was also found to be (inversely)related to the laser repetition frequency, because of refractive index gradients set up in the methane by virtue of the energy deposited in the gas by the Raman process. Work is in progress to run the system at higher repetition frequency with enhanced conversion efficiency.

References

[1] This research was supported primarily by the University of Maryland and by NASA–Goddard Space Flight Center (NAG-5-1114), and partly by NASA-Langley Research Center (NCC1-25).

[2] R. M. Measures, Laser Remote Sensing, John Wiley & Sons, New York (1984).

[3] E.M. Patterson, D.W. Roberts, G.G. Gimmestad, Proc. Conf. of Laser and Electro-optics (CLEO '89), Baltimore, Maryland (April, 1989).

[4] J.T. Lin, Proc. Intern. Laser Conf.(LASER '86),Orlando, Florida (November, 1986).

[5] C.G. Parazzoli, W.W. Buchman, R.D. Stultz, IEEE J. Quantum. Electron. QE-24, 872 (1988).

[6] Z. Chu, U.N. Singh, T.D. Wilkerson, accepted for publication in Optics Communication (1990).
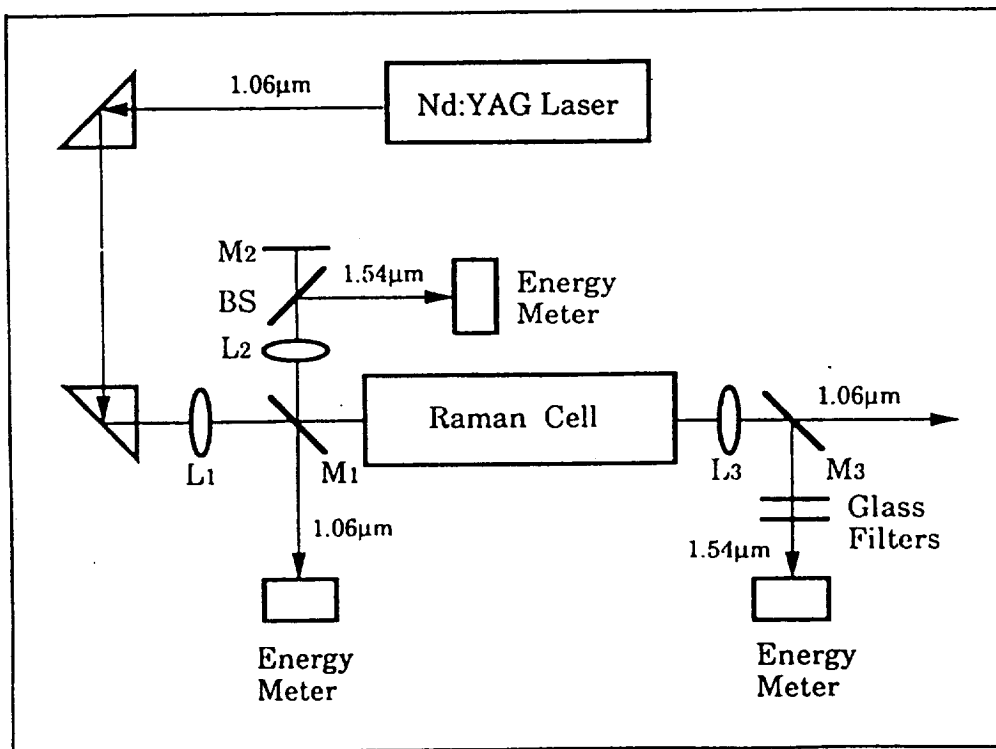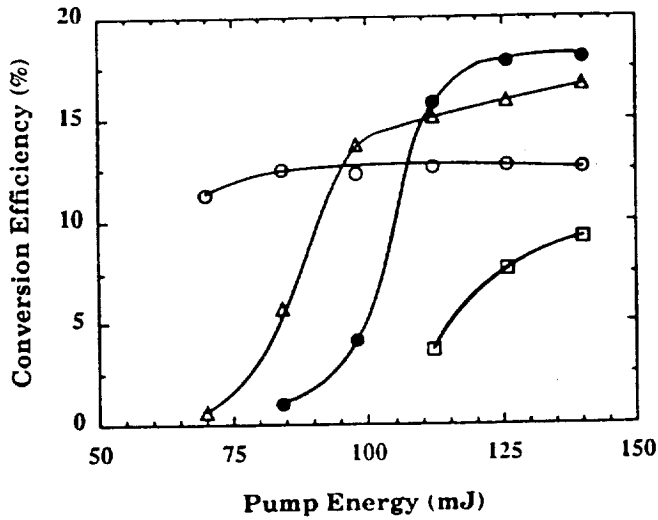
Figure 1. Experimental setup.

Figure 2. Energy conversion efficiency to the injection-seeded forward first Stokes as a function of pump energy for different gas pressures:
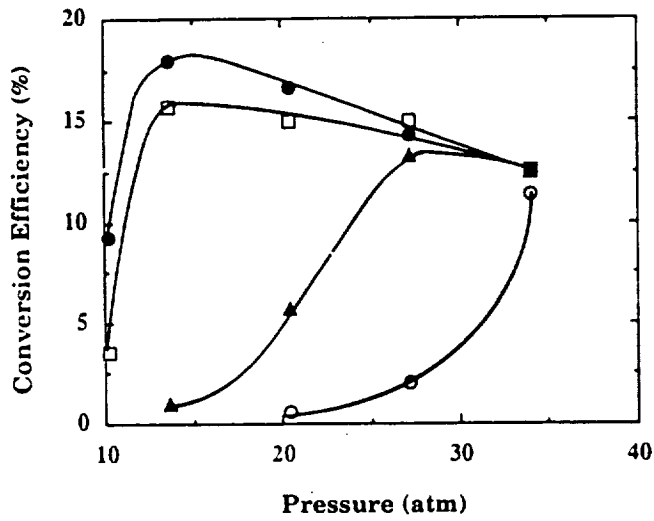
□, 10atm; ●, 14atm; △, 20atm; ○, 34atm

Figure 3. Conversion efficiency to the injection-seeded first Stokes as a function of gas pressure for different pump energy:
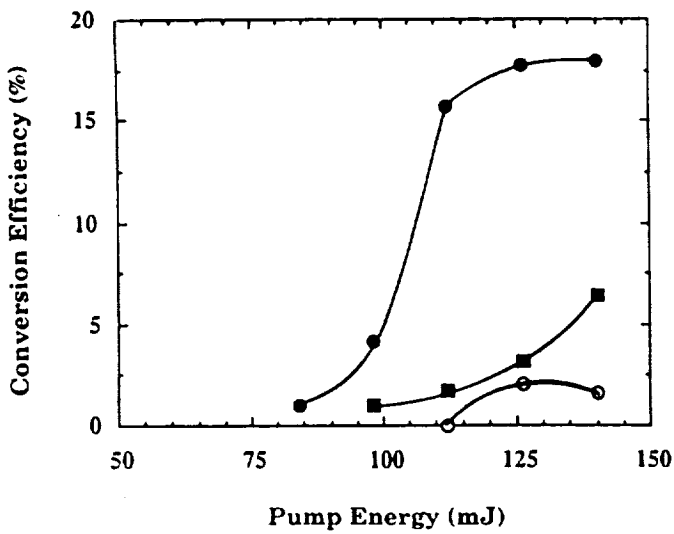
●, 140mJ; □, 112mJ; ▲, 84mJ; ○, 70mJ.

Figure 4. Conversion efficiency for the injection-seeded first Stokes (●) as a function of pump energy for a gas pressure of 14 atm. As a comparision, the conversion efficiency for the backward first Stokes seed (○) and the forward first Stokes in the unseeded case (■) are also shown.

NASA
FORMAL
REPORT